

A Novel Cough Strength Evaluation Method via Cough Sounds

(咳嗽音を用いた新しい咳嗽力評価法の提案)

by

Yasutaka Umayahara

Graduate School of Engineering

Hiroshima University

March, 2019

Contents

| | | |
|------------------|---|----------|
| Chapter 1 | Introduction | 1 |
| 1.1 | Background and Purpose | 1 |
| 1.2 | Related Works | 3 |
| 1.2.1 | Importance of cough | 3 |
| 1.2.2 | Conventional measurement method of cough ability and its disadvantage | 5 |
| 1.2.3 | Cough sound analysis | 6 |
| 1.3 | Outline of the Dissertation | 7 |
| Chapter 2 | Estimation of Cough Peak Flow via Cough Sounds | 9 |
| 2.1 | Introduction | 9 |
| 2.2 | Cough peak flow (CPF) estimation model | 10 |
| 2.2.1 | Estimation formula of CPF using cough sounds | 10 |
| 2.2.2 | Relationship between CPF and cough peak sound pressure level (CPSL) by non-linear regression analysis | 11 |
| 2.2.3 | Verification of microphone installation method | 12 |
| 2.3 | Accuracy of estimated CPF via cough sounds (CPS) | 13 |
| 2.3.1 | Effect of microphone distance from sound source | 13 |
| 2.3.2 | Effect of height | 13 |

| | | |
|------------------|--|-----------|
| 2.3.3 | Effect of gender | 14 |
| 2.3.4 | Comparison between the proposed model and polynomial functions | 14 |
| 2.4 | Results | 20 |
| 2.5 | Discussion | 28 |
| 2.6 | Concluding Remarks | 32 |
| | | |
| Chapter 3 | Effects of Microphone Type on Cough Strength Estimation | |
| | Accuracy | 33 |
| 3.1 | Introduction | 33 |
| 3.2 | Experimental methods | 35 |
| 3.3 | Results | 39 |
| 3.4 | Discussion | 45 |
| 3.5 | Concluding Remarks | 46 |
| | | |
| Chapter 4 | A Mobile Cough Strength Evaluation Device via Cough Sounds | 49 |
| 4.1 | Introduction | 49 |
| 4.2 | Proposed device | 51 |
| 4.2.1 | Model | 51 |
| 4.2.2 | Measurement protocol and preprocessing for cough sounds | 51 |
| 4.2.3 | User interface software | 53 |
| 4.3 | Experiments | 56 |
| 4.3.1 | Participants | 56 |
| 4.3.2 | Methods | 57 |
| 4.4 | Results | 60 |
| 4.5 | Discussion | 69 |

| | | | |
|------------------|------------------------|-------|------------|
| 4.6 | Concluding Remarks | | 71 |
| Chapter 5 | Conclusions | | 73 |
| | Bibliography | | 77 |
| | Acknowledgments | | xc1 |

List of Figures

- 1.1 Normal cough mechanism. (a) Inspiratory phase. (b) Compressive phase. (c) Expulsive phase. 3
- 1.2 Cough peak flow measurement device. (a) Spirometer. (b) Peak flow meter. (c) Flow sensor. (d) Face mask. (e) infection control filter. 6
- 1.3 Conventional method of cough strength measurement. Cough peak flow is assessed using a spirometer. 6
- 2.1 Experimental methods. (a) Experiment 1 method. The cough flow measurement is performed with the participants in a sitting position. The participants wear a face mask with an attached flow sensor. Two microphones are installed 30 cm from the point of face mask contact with the face. Microphone 1 is attached to the flow sensor and microphone 2 is fixed to the microphone stand. (b) Experiment 2 method. Microphones are installed 20 cm, 30 cm, 40 cm, 50 cm and 60 cm away from the point of face mask contact with the face. (c) In-ear microphone. The in-ear microphone was used in experiment 3 and fixed at the right external auditory canal. (d) Mini speech microphone. The mini speech microphone was used in experiment 3. (e) Smartphone microphone: The smartphone microphone was used in experiment 3. 12

- 2.2 Examples of cough flow and cough sounds measured by microphones 1 and 2. (a) Experimental data of cough flow signals in experiment 1. *CPF*, cough peak flow. (b) Experimental data of cough sound signals measured by microphone 1 attached to the flow sensor in experiment 1. (c) Experimental data of cough sound signals measured by microphone 2 fixed to the microphone stand in experiment 1. (d) Absolute values of cough sound measured by microphone 1. (e) Envelope of cough sound signals calculated from the absolute cough sound values measured by microphone 1. *CPSL* is defined as the maximum value of the envelope. 18
- 2.3 Estimation accuracy of Equation (2.7) calculated from the experimental data measured by microphone 1 attached to the flow sensor. (a) Relationship of *CPF* and *CPSL_{microphone1}*. The solid lines represent the regression curves derived by fitting the coefficients in the proposed model using the Levenberg-Marquardt method based on *CPF* and *CPSL_{microphone1}*. The dotted lines represent 95% confidence bands. *CPF*, cough peak flow; *CPSL_{microphone1}*, cough peak sound pressure level by microphone 1. (b) Relationship between *CPF* and *CPS_{microphone1}*. *CPS_{microphone1}*, estimated cough peak flow calculated from *CPSL_{microphone1}*. 21
- 2.4 Estimation accuracy in each measurement condition. (a–e): Scatter plots of the measured data and the regression results of the proposed model: *CPSL_{20 cm to 60 cm}*, cough peak sound pressure level measured by each microphone installed 20 cm, 30 cm, 40 cm, 50 cm and 60 cm from

- the point of face mask contact with the face; $CPS_{20\text{ cm to }60\text{ cm}}$, estimated cough peak flow calculated by $CPSL_{20\text{ cm to }60\text{ cm}}$. Solid lines represent regression lines derived from CPF and $CPSL$. The variation around the identity line is visibly reduced in graphs (a, b). 23
- 2.5 Comparison of the absolute error between each measurement condition. CPF , cough peak flow; CPS , estimated cough peak flow; * $P < 0.001$ 24
- 2.6 The results of experiment 3. CPF , cough peak flow; CPS_{in-ear} , estimated CPF calculated from cough sound measured using the in-ear microphone; $CPS_{mini-speech}$, estimated CPF calculated from cough sound measured using the mini speech microphone; $CPS_{smartphone}$, estimated CPF calculated from cough sound measured using the smartphone microphone. (a) Relationship between CPF and CPS_{in-ear} . (b) Relationship between CPF and $CPS_{mini-speech}$. (c) Relationship between CPF and CPS_{smart} 25
- 2.7 Bland-Altman plot of the measured and estimated cough peak flow. CPF , cough peak flow; CPS , estimated cough peak flow. (a) CPS estimated using our proposed model of Equation (2.1). (b) CPS estimated using Equation (2.4). Blue and black dots represent the difference between CPF and CPS . Bold black solid lines represent the mean difference between CPF and CPS . Green dotted lines represent the mean difference ± 2 standard deviation bands. Red lines represent

| | | |
|-----|---|----|
| | the approximate straight line of the difference between <i>CPF</i> and <i>CPS</i> and the mean of <i>CPF</i> and <i>CPS</i> | 28 |
| 3.1 | Types of microphones and measurement position. (a) In-ear microphone. (b) Mini speech microphone. (c) Smartphone microphone. | 37 |
| 3.2 | Results of non-linear regression analysis. (a) In-ear microphone. Non-linear regression using Equation (3.1). (b) Mini speech microphone. Non-linear regression using Equation (3.1). (c) Smartphone microphone. Non-linear regression using Equation (3.1). (d) In-ear microphone. Non-linear regression using Equation (3.2). (e) Mini speech microphone. Non-linear regression using Equation (3.2). (f) Smartphone microphone. Non-linear regression using Equation (3.2). | 40 |
| 3.3 | Results of the rank correlation coefficient of the Speaman analysis. (a) In-ear microphone. CPS_{in-ear} was calculated using (3.1). (b) Mini speech microphone. $CPS_{mini-speech}$ was calculated using (3.1). (c) Smartphone microphone. $CPS_{smartphone}$ was calculated using (3.1). (d) In-ear microphone. CPS_{in-ear} was calculated using (3.2). (e) Mini speech microphone. $CPS_{min-speech}$ was calculated using (3.2). (f) Smartphone microphone. $CPS_{Samarthphone}$ was calculated using (3.2). | 42 |
| 3.4 | Results of the Bland-Altman method for assessing agreement between <i>CPS</i> and <i>CPF</i> . (a) In-ear microphone. (b) Mini speech microphone. (c) Smartphone microphone. (d) In-ear microphone. (e) Mini speech | |

| | | |
|-----|--|----|
| | microphone. (f) Smartphone microphone. solid line: mean difference; dashed line: 95% confidence interval of difference. | 43 |
| 3.5 | Graph comparing the relative errors between different microphone types. Friedman test showed that there was no significant difference between the relative errors ($P = 0.315$). | 44 |
| 4.1 | Cough sound measurement protocol and software configuration. <i>CPS</i> represents the cough peak flow estimated using cough sounds. (a) The posture of a user while recording cough sounds. (b) The user interface for editing a personal profile. (c) The flow chart for cough sound preprocessing and cough peak flow (CPF) estimation. (d) The results display that demonstrates the graphs resulting from signal preprocessing and CPF estimation. | 53 |
| 4.2 | Editorial part. This screen prompts the user to complete their personal profile. BMI, body mass index, $BMI = \text{body weight} / \text{height}^2$; VC, vital capacity; FVC, forced vital capacity; FEV_1 , forced expiratory volume in 1 s; RSST, repetitive saliva swallowing test. | 54 |
| 4.3 | Results display part. The blue solid line represents the measured cough sound signal. The light blue solid line represents the rectified sound signal. The purple solid line represents the moving average with a time window of 20 ms. The red dot represents the maximum point of the moving average. | 55 |

- 4.4 Estimation accuracy of $CPS_{proposed}$ and $CPS_{previous}$. (a) The CPF estimated by the proposed model ($CPS_{proposed}$) against the measured CPF. (b) Plot of the CPF estimated by the previous model ($CPS_{previous}$) against the measured CPF. The red and blue circles represent the elderly and young participants, respectively. The linear regression lines are drawn for the groups of young and elderly participants, and the corresponding equations are shown in the upper part of each figure, where the green letters indicate the equation of the regression line for all participants. The right lower side shows the correlation coefficients and P values for each participant group. 63
- 4.5 Comparison of the absolute error between the proposed and previous models. (a) Young participants, $n = 33$. (b) Elderly participants, $n = 25$. (c) All participants, $n = 58$ 63
- 4.6 Bland-Altman plots of the measured and estimated CPFs. (a) The estimation accuracy of the proposed model ($CPS_{proposed}$). (b) The estimation accuracy of the previous model ($CPS_{previous}$). The horizontal line is the mean of the measured CPF and estimated cough peak flow (CPS_x). The vertical line represents the difference between the measured CPF and CPS_x . The bold black solid lines represent the mean differences between the CPF and CPS_x , and the red dotted lines represent the mean differences ± 2 standard deviations. 64
- 4.7 Estimation accuracy of CPS_{height} . (a) CPS_{height} against the measured CPF. The linear regression lines are drawn for the young and elderly

- participant groups, and the corresponding equations are shown in the upper part of each figure, where the green indicates the equation of the regression line for all participants. The right lower part shows the correlation coefficients and p values for each participant group. (b) Bland-Altman plot of the measured CPF and CPS_{height} . The horizontal line is the mean of the measured CPF and CPS_{height} . The vertical line represents the difference between the measured CPF and CPS_{height} . The bold black solid lines represent the mean difference between the measured CPF and each CPS_{height} , and the red dotted lines represent the mean difference ± 2 standard deviation bands. 66
- 4.8 Comparison of the absolute error of the proposed and height models. $n = 58$ 67
- 4.9 Examples of elderly participants. The grey line represents the measured cough sound signal. The light blue solid line represents the bandpass-filtered and rectified sound signal. The purple solid line represents the moving average with a time window of 20 ms. The red circle represents the maximum point of the moving average. (a) Example of a 77-year-old female with a measured CPF below the reference value of 270 L/min. The respiratory function test showed slightly low values of %VC = 83.5% and FEV₁/FVC = 83.0%, but these values exceed the reference value. (b) Example of a 70-year-old male with a measured CPF above the reference value of 270 L/min. The respiratory function test showed normal values of %VC = 91.6% and FEV₁/FVC = 94.9%. 68

List of Tables

| | | |
|------|--|----|
| 2.1. | Characteristics of the participants. | 16 |
| 2.2. | Relationship between cough peak flow and cough peak sound pressure level using Equations (2.3)–(2.4). | 27 |
| 3.1. | Results of non-linear resression. | 41 |
| 3.2. | Results of the rank correlation coefficient of Spearman. | 43 |
| 4.1. | Characteristics of the participants. | 57 |
| | Values presented are the number of participants or the mean \pm S.D. of the corresponding parameters, unless otherwise stated. BMI, body mass index; VC, vital capacity; %VC, vital capacity expressed as a percentage of the predicted value; FEV ₁ , forced expiratory volume in 1 s; FVC, forced vital capacity. | |
| 4.2. | Determined parameters. | 61 |

Abbreviations and Acronyms

| | |
|----------------------------|--|
| BMI | Body mass index |
| CPF | Cough peak flow |
| CPS | Estimated cough peak flow via cough sounds |
| CPS _{microphone1} | Estimated cough peak flow calculated from the cough sound measured using microphone 1 |
| CPS _{microphone2} | Estimated cough peak flow calculated from the cough sound measured using microphone 2 |
| CPS _{20cm} | Estimated cough peak flow calculated from the cough sound measured using a microphone installed 20 cm away from the point of face mask contact with the face |
| CPS _{30cm} | Estimated cough peak flow calculated from the cough sound measured using a microphone installed 30 cm away from the point of face mask contact with the face |
| CPS _{40cm} | Estimated cough peak flow calculated from the cough sound measured using a microphone installed 40 cm away from the point of face mask contact with the face |
| CPS _{50cm} | Estimated cough peak flow calculated from the cough sound measured using a microphone installed 50 cm |

| | |
|-----------------------------|--|
| | away from the point of face mask contact with the face |
| CPS _{60cm} | Estimated cough peak flow calculated from the cough sound measured using a microphone installed 60 cm away from the point of face mask contact with the face |
| CPS _{in-ear} | Estimated cough peak flow calculated from the cough sound measured using an in-ear microphone |
| CPS _{mini-speech} | Estimated cough peak flow calculated from the cough sound measured using a mini-speech microphone |
| CPS _{smartphone} | Estimated cough peak flow calculated from the cough sound measured using a smartphone microphone |
| CPSL | Cough peak sound pressure level |
| CPSL _{microphone1} | Cough peak sound pressure level measured using microphone 1 |
| CPSL _{microphone2} | Cough peak sound pressure level measured using microphone 2 |
| CPSL _{20cm} | Cough peak sound pressure level measured using a microphone installed 20 cm away from the point of face mask contact with the face |
| CPSL _{30cm} | Cough peak sound pressure level measured using a microphone installed 30 cm away from the point of face mask contact with the face |

| | |
|-----------------------------|--|
| CPSL _{40cm} | Cough peak sound pressure level measured using a microphone installed 40 cm away from the point of face mask contact with the face |
| CPSL _{50cm} | Cough peak sound pressure level measured using a microphone installed 50 cm away from the point of face mask contact with the face |
| CPSL _{60cm} | Cough peak sound pressure level measured using a microphone installed 60 cm away from the point of face mask contact with the face |
| CPSL _{in-ear} | Cough peak sound pressure level measured using an in-ear microphone |
| CPSL _{mini-speech} | Cough peak sound pressure level measured using a mini-speech microphone |
| CPSL _{smartphone} | Cough peak sound pressure level measured using a smartphone microphone |
| FEV ₁ | Forced expiratory volume in 1 s |
| FEV ₁ /FVC | Forced expiratory volume in 1 second as percent of forced vital capacity |
| FVC | Forced vital capacity |
| RSST | Repetitive saliva swallowing test |

VC Vital capacity

%VC Vital capacity as percent of predicted

Chapter 1

Introduction

1.1 Background and Purpose

According to a survey by the Ministry of Health, Labor and Welfare on overtaking stroke, pneumonia is the third leading cause of death in Japan [1], and 66.8% of patients hospitalized for pneumonia are diagnosed with aspiration pneumonia [2]. A recent study among Japanese elderly people has shown that one of the risk factors for aspiration pneumonia is sputum suctioning [3]. Although repeated aspiration occurs due to dysphagia, pneumonia rarely develops if the aspirated substance is completely expelled from the airway by coughing. Thus, assessment of cough ability is important to identify the risk of aspiration pneumonia. Cough peak flow (CPF) is used to assess cough strength. However, there are some patients, including elderly patients with dementia, whose cough strength cannot be measured using the current device due to discomfort upon attachment [4]. Thus, cough sound can be examined to develop a novel simple cough strength evaluation method. Several studies have reported that the relationship between air flow and the amplitude of breath sound is

linear at a high flow rate condition [5,6]. It has also been reported that the sound amplitude during inspiration is proportional to the square of the air flow velocity at the mouth [7]. These studies indicate a relation between breath sound and air flow. Thus, in this study, we hypothesized that cough sounds are associated with cough flow and proposed a novel cough strength measurement method and mobile device using a CPF estimation model via cough sound. This study also investigated the optimal cough sound measurement method and the influence of participant height, gender, microphone type and age on the accuracy of the estimated CPF via cough sound (CPS). We compared the proposed model with polynomial functions to verify its effectiveness.

To achieve the above objective, this study focused on the following areas:

- **Estimation of cough peak flow via cough sounds**

A CPF estimation model was formulated via cough sound. The relationship between cough sounds and cough flows was investigated using non-linear regression analysis (the Levenberg–Marquardt method).

- **Cough strength estimation accuracy**

In this study, we conducted experiments to verify the effects of the measurement condition of cough sound, microphone type, participant's height, gender, body weight, BMI and age on CPF estimation accuracy.

- **Mobile cough strength evaluation device via cough sounds**

A user interface for mobile devices such as a smartphone was developed to record cough sounds and estimate cough strength in elderly people

using the proposed method.

1.2 Related Works

1.2.1 Importance of cough

Cough can be an important defence mechanism to help clear excessive secretions and foreign substance from airways [8,9]. Figure 1.1 shows a normal cough mechanism. Cough is a three-phase expulsive motor action characterised by an inspiratory effort (inspiratory phase), followed by a forced expiratory effort against a closed glottis (compressive phase) and then opening of the glottis and rapid expiratory airflow (expulsive phase) [10]. In addition to mobilizing and expelling secretions, high pressures generated during a cough may be an important factor in re-expanding lung tissue [11].

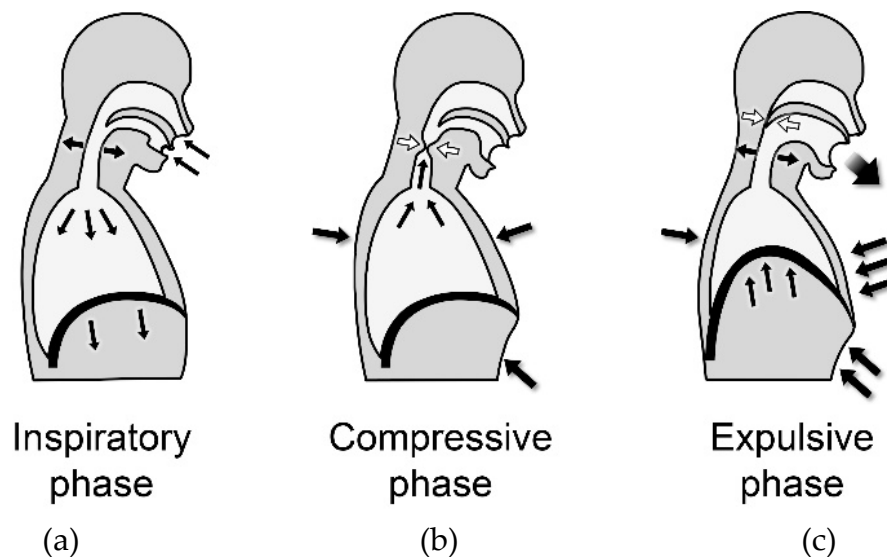


Figure 1.1 Normal cough mechanism. (a) Inspiratory phase. (b) Compressive phase. (c) Expulsive phase.

There are several ways to evaluate cough. Cough visual analogue scores [12,13], cough specific health status questionnaires [9,14,15], cough reflex sensitivity measurement [16] and cough monitors [17] have been proposed as potential tools to assess cough. The inhalation cough challenge permits measurement of the sensitivity of cough reflex and assessment of the antitussive effects of specific therapies [18]. Cough monitor can assess cough frequency associated with cough sensitivity and cough specific health status in patients with chronic cough [19]. Cough strength is associated with predicting extubation in patients with weak cough and high possibility of re-intubation [20-22]. CPF (sometimes called PCF) is commonly used to assess cough strength [23-25], and also described in guidelines published by various academic societies [26-28]. Previous studies reported that at least 160 L/min of CPF is the minimum required to clear airway debris and necessary for the successful extubation or tracheostomy tube decannulation in patients with neuromuscular disease irrespective of ability to breathe [29,30]. Moreover, patients with a maximum assisted CPF below 270 L/min were also considered to be at risk of upper respiratory tract infections associated with respiratory failure [31]. In recent years, CPF has been investigated in elderly people by many researchers and has attracted attention as an indicator reflecting the airway clearance ability and aspiration pneumonia risk of the elderly [32,33]. Aspiration is an independent risk factor associated with the development of pneumonia [34], and a previous study has shown that 66.8% of patients hospitalized for pneumonia are diagnosed with aspiration pneumonia [2]. Therefore, early detection of aspiration pneumonia is critical for treatment. Ebihara et al. (2016) suggested that research efforts should focus on approaches to improve coughing

dysfunction, rather than develop new antibiotics, to decrease mortality due to aspiration pneumonia in the elderly [35]. To prevent aspiration pneumonia, the evaluation of cough ability is as important as that of swallowing. A CPF level lower than 242 L/min indicates the development of pulmonary complications in dysphagic patients with persistent tracheobronchial aspiration [33].

1.2.2 Conventional measurement method of cough ability and its disadvantage

In previous studies, CPF was measured using various devices, such as peak flow meters, spirometers and pneumotachographs (Figure 1.2). However, some medical facilities do not provide these devices [22], and a semiquantitative cough strength assessment was sometimes used in some studies [36,37]. Moreover, the complex setup of the device, including firmly attaching the facemasks and infection control filters on the patient, imposes burdens on both patients and their caregivers (Figure 1.3). In addition, the measured CPF value can vary depending on the type of facemask and filter. Furthermore, the mask, which is firmly attached to the patient's face to prevent air leakage, makes it difficult for the subject to cough naturally and voluntarily.

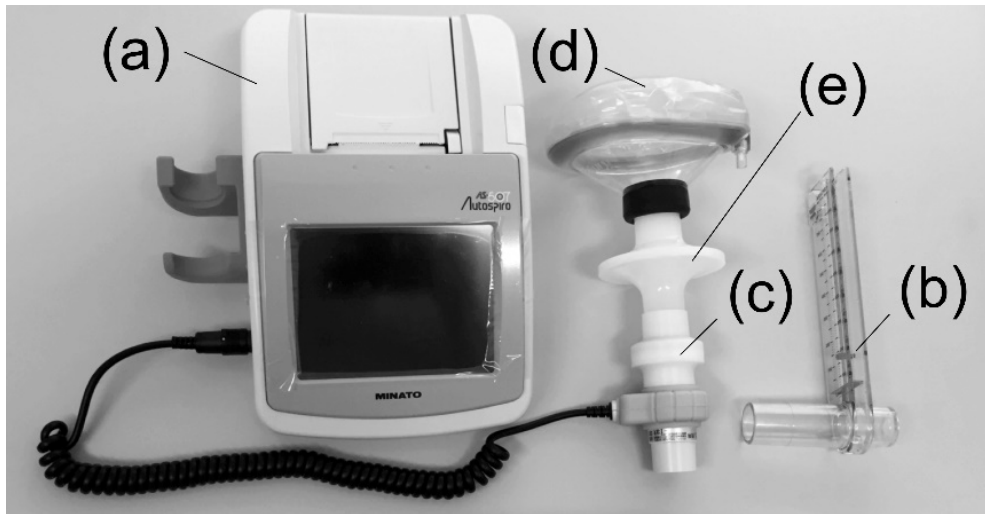


Figure 1.2 Cough peak flow measurement device. (a) Spirometer. (b) Peak flow meter. (c) Flow sensor. (d) Face mask. (e) infection control filter.



Figure 1.3 Conventional method of cough strength measurement. Cough peak flow is assessed using a spirometer.

1.2.3 Cough sound analysis

Cough commonly has many characteristics such as non-productive cough without sputum, productive cough with sputum, a mixture of the two, temporary or not, and changing properties from the acute phase to the chronic

phase. In previous studies, cough characteristics are analysed based on the subjective interpretation of cough sound recordings and analysis of spectrograms [38-42]. Recording cough sound using a free-air microphone has been described as early as 1960 [43,44]. The cough sound signals were normally recorded using various microphones attached to the neck, the chest wall, or over the trachea [40]. Moreover, an automated classifier proposed in a previous study can determine whether human coughs generated by a given individual are spontaneous or voluntary [45], and recorded free field cough sounds can be used to identify several distinguishing features of acoustic signals [46]. These studies proposed methods to monitor cough frequency using a microphone, but not to monitor the cough strength. If the assessment of cough strength by cough sounds is feasible, it can be applied to patients in whom cough peak flow measurements using the current method are difficult. However, the relationship between cough flow and cough sounds has not yet been clarified.

1.3 Outline of the Dissertation

The thesis is organized as follows:

In Chapter 2, the development of a novel cough strength evaluation method using cough sounds is described and an exponential model to estimate CPF from the cough peak sound pressure level (CPSL) is presented. Moreover, the effects of the measurement condition of cough sound, participant's height and gender on CPF estimation accuracy were verified.

Chapter 3 describes experiments conducted to verify the effects of three types of

microphones (ear-in microphone, mini speech microphone, and smartphone built-in microphone) on CPF estimation accuracy.

In Chapter 4, the proposed CPF estimation model that takes into account the relationship between CPFs and cough sounds as well as age, body weight and BMI is presented. In addition, a user interface that incorporates the proposed CPF estimation model in mobile devices and enables cough sound recording, immediate CPF estimation, and estimated CPF history management was developed for future applications in clinics and home.

Finally, Chapter 5 presents the conclusion of the dissertation and outlines some challenges and future work.

Chapter 2

Estimation of Cough Peak Flow via Cough Sounds

2.1 Introduction

CPF is a measurement commonly used to evaluate cough strength, which reflects the ability to expel airway secretions [24,25,30,47-50] and can predict extubation [20,30] and reintubation outcomes [21,51,52]. Values of CPF below 160 L/min have been associated with ineffective airway clearance [24,29,30] and patients that can generate a CPF of more than 270 L/min have little risk of developing respiratory failure during upper respiratory tract infections [31]. In previous studies, CPF was measured using various devices, such as flow meters, spirometers and pneumotachographs. However, some medical facilities do not provide these devices [14]. Moreover, the complex setup of the device, including firmly attaching the facemasks and infection control filters on the patient [25], imposes burdens on both patients and their caregivers. In addition, the measured CPF value can vary depending on the type of facemask and filter.

Therefore, we propose a novel simple system for evaluating cough

ability using cough sounds without the use of the facemask or the filter. Several previous studies have proposed methods to monitor cough frequency using a microphone [18,19,53-58], but not to monitor cough ability. If the assessment of cough ability by cough sounds is feasible, it can be applied to patients in whom cough peak flow measurements using the current method are difficult. However, the relationship between cough flow and cough sounds has not yet been clarified.

In this study, we tested a hypothesis that cough sounds are associated with cough flow. Experiments were conducted to determine the optimal cough sound measurement method and to investigate the influence of microphone type and participant's height and gender on the accuracy of the *CPF* estimated via cough sounds (*CPS*) in young healthy participants. The effectiveness of the proposed model was also verified by comparison with polynomial functions.

2.2 Cough peak flow (CPF) estimation model

2.2.1 Estimation formula of CPF using cough sounds

This study proposes a CPF estimation model to assess cough strength. Details of the proposed model are described in this section.

The proposed model is expressed by the following equation:

$$CPF = \alpha(e^{\beta \cdot CPSL} - 1), \quad (2.1)$$

where α and β are constants and the *CPSL* represents the cough peak sound pressure level.

2.2.2 Relationship between CPF and cough peak sound pressure level (CPSL) by non-linear regression analysis

The maximum cough sound was used because previous studies have identified a clear correlation between the peak flow and the maximal absolute breath sound [5,59]. The coefficients in the proposed model, that is Equation (2.1), was predetermined by non-linear regression analysis (the Levenberg-Marquardt method) using the mean square error between *CPS* and the measured *CPF* as the evaluation function. *CPSL* represents the cough peak sound pressure level. This model indicates that the relationship between *CPF* (*CPS*) and *CPSL* can be defined by a logarithm function. The next section describes the pre-processing method used to derive *CPSL* from cough sounds, which can be measured using a microphone.

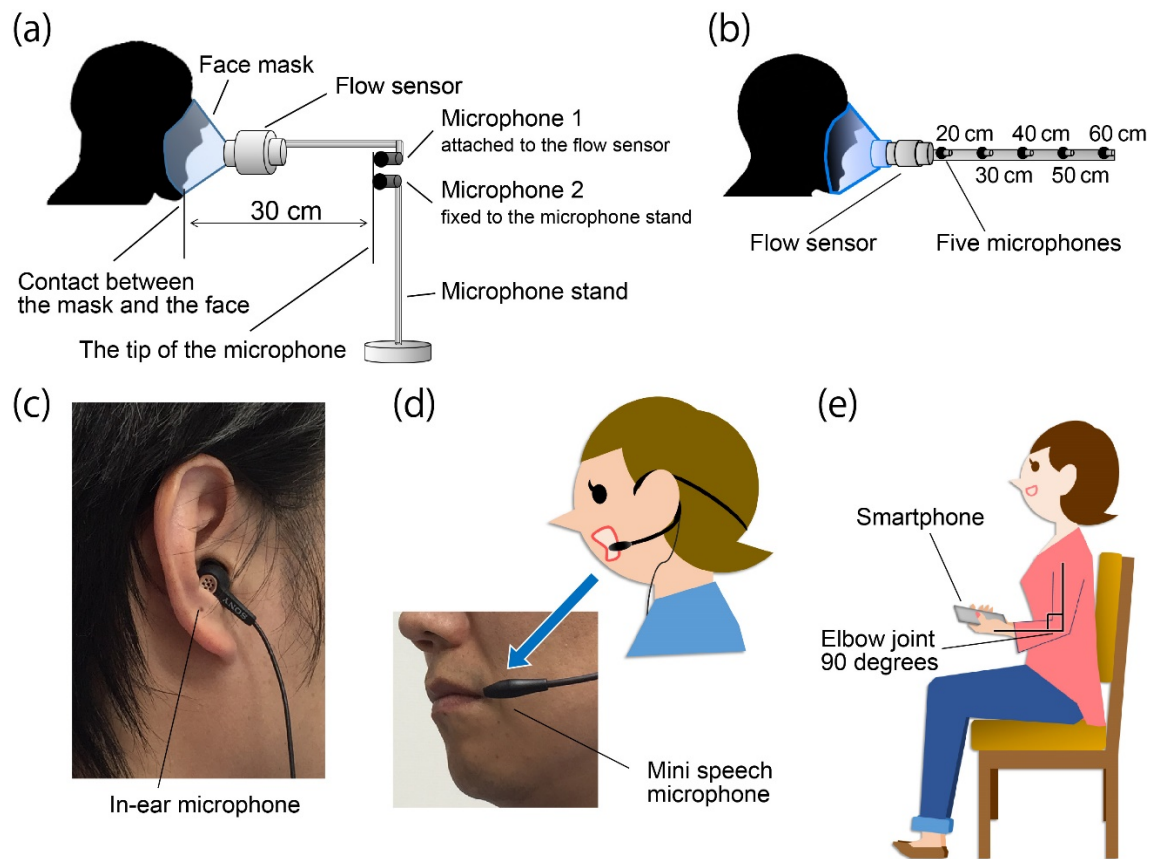


Figure 2.1 Experimental methods. (a) Experiment 1 method. The cough flow measurement is performed with the participants in a sitting position. The participants wear a face mask with an attached flow sensor. Two microphones are installed 30 cm from the point of face mask contact with the face. Microphone 1 is attached to the flow sensor and microphone 2 is fixed to the microphone stand. (b) Experiment 2 method. Microphones are installed 20 cm, 30 cm, 40 cm, 50 cm and 60 cm away from the point of face mask contact with the face. (c) In-ear microphone. The in-ear microphone was used in experiment 3 and fixed at the right external auditory canal. (d) Mini speech microphone. The mini speech microphone was used in experiment 3. (e) Smartphone microphone: The smartphone microphone was used in experiment 3.

2.2.3 Verification of microphone installation method

Experiments 1 was conducted to determine the optimal cough sound measurement method. Cough sounds were measured using two microphones

(AT9903, Audio-Technica Corporation, Tokyo, Japan), simultaneously with cough flow. The sensitivity of the microphones was -42 dB (0 dB = 1 V/1 Pa, 1 kHz). Both microphones were installed 30 cm away from the point of face mask contact with the face, but using different installation methods to test their efficacy; that is, microphone 1 was fixed to the flow sensor [38], whereas microphone 2 was fixed to the microphone stand, as shown in Figure 2.1a.

2.3 Accuracy of Estimated CPF via Cough Sounds (CPS)

2.3.1 Effect of microphone Distance from Sound Source

Experiment 2 was conducted to determine the effect of the microphone distance from the sound source, that is, the participant's mouth, on the accuracy of the estimated *CPF* via *CPS* in young healthy participants. Cough sounds were simultaneously measured using five microphones of the same type as in experiment 1. Each microphone was installed at 20 cm, 30 cm, 40 cm, 50 cm and 60 cm away from the point of face mask contact with the face (Figure 2.1b).

2.3.2 Effect of Height

We hypothesized that the coefficient α increases proportionally with height and we represented α using a linear term related to height, as in the following equation:

$$CPF = (\alpha_1 \cdot h + \alpha_2)(e^{\beta \cdot CPSL} - 1), \quad (2.2)$$

where h is the participant's height and α_1 , α_2 and β are constants. Data from microphone 1 used in Experiment 1 were also used for this experiment.

2.3.3 Effect of Gender

To determine the effect of gender on CPS , we divided the participants into male and female groups and coefficients α and β were calculated for each group using the Levenberg–Marquardt method. Moreover, Mann–Whitney's U test was used to compare the coefficients between the two groups. Data recorded from microphone 1 in experiment 1 were used for this analysis.

2.3.4 Comparison Between the Proposed Model and Polynomial Functions

To verify the efficacy of the proposed model, we compared the model with first- to fourth-order polynomial functions, as in the following equations:

$$CPF = \alpha_3 \cdot CPSL, \quad (2.3)$$

$$CPF = \alpha_4 \cdot CPSL^2 + \alpha_5 \cdot CPSL, \quad (2.4)$$

$$CPF = \alpha_6 \cdot CPSL^3 + \alpha_7 \cdot CPSL^2 + \alpha_8 \cdot CPSL, \quad (2.5)$$

$$CPF = \alpha_9 \cdot CPSL^4 + \alpha_{10} \cdot CPSL^3 + \alpha_{11} \cdot CPSL^2 + \alpha_{12} \cdot CPSL, \quad (2.6)$$

where α_3 – α_{12} are constants. The Levenberg–Marquardt method was also used to determine the coefficient in the equations and the coefficient of determination,

and the 95% CIs were calculated. Data from microphone 1 in Experiment 1 were used for this analysis.

Materials and Methods

This study was conducted in accordance with the amended Declaration of Helsinki. The Hiroshima Cosmopolitan University Institutional Review Board (No. 2015031) approved the protocol and we obtained written informed consent from all participants for participation in the study and for the use of identifying information/images in online open-access publication.

Participants

A total of 73 young healthy participants who were screened for the absence of pulmonary illness (forced expiratory volume in 1 s of at least 70% of predicted) with no history of pulmonary disease were included in this study. The participants were non-smokers, were not taking any long-term prescription medications and did not have any other medical illnesses. The mean \pm standard deviation age of the participants was 21.0 ± 1.2 years (range, 20 to 28 years). Table 2.1 presents the baseline characteristics of the participants. It should be noted that the mean values (standard deviations) of body weight and BMI of Japanese who are over 20 years old are 66.8 (10.6) kg and 23.7 (3.2) % and 53.2 (8.7) kg and 22.4 (3.4) % in males and females, respectively [60]; these values are almost the same as those of the participants in experiment 1.

Table 2.1 Characteristics of the participants.

| Variable | Experiment 1 (<i>n</i> = 33) | Experiment 2 (<i>n</i> = 7) | Experiment 3 (<i>n</i> = 33) |
|--|--------------------------------------|--|--|
| Age, years | 20.7 ± 1.0 | 22.0 ± 2.8 | 21.3 ± 0.4 |
| Male gender, <i>n</i> | 21 | 5 | 20 |
| Height, cm | 167 ± 7.9 | 167 ± 7.5 | 165 ± 8.4 |
| Body weight, kg (male, female) | 61.5 ± 12 (66.0 ± 12, 53.7 ± 5.4) | 58.7 ± 9 (61.0 ± 7.6, 53.0 ± 11.3) | 58.5 ± 11 (64.5 ± 11.3, 51.0 ± 6.2) |
| BMI, kg/m ² (male, female) | 21.9 ± 3.2 (22.4 ± 3.6, 21 ± 2.1) | 22.0 ± 2.8 (21.2 ± 2.0, 20.3 ± 2.2) | 21.3 ± 0.5 (21.4 ± 0.6, 20.9 ± 0.5) |

Values presented as mean ± standard deviation.

Cough Flow Measurements

Figure 2.1a shows the cough flow measurement method that was performed with the participants in a sitting position for all experiments. Participants wore a face mask with a flow sensor (Mobile Aeromonitor AE-100i; Minato Medical Science Co., Ltd., Osaka, Japan) attached. The measurement range of the flow sensor was 0–840 L/min and the measurement accuracy was within 3% of the indicated value. The cough flow signal was digitized using a 16-bit analogue-to-digital converter (PowerLab 16/35, ADInstruments, Inc., Dunedin, New Zealand) at a sampling rate of 100-kHz set by analytical software (LabChart version 8, ADInstruments, Inc., Bella Vista, Australia). CPF was calculated from the maximal value of cough flow data obtained under different experimental conditions.

Cough Sound Measurements

Experiment 3: Cough sounds were measured using three types of microphones. An electret condenser microphone (ECM-TL3; Sony Corporation, Tokyo, Japan) (in-ear microphone) was attached to the right ear canal to measure cough sounds from the right external auditory canal, as shown in Figure 2.1c. The sensitivity of the microphone was -35.0 dB (0 dB = 1 V/1 Pa, 1 kHz). A headset mini speech microphone (ECM-322BMP; Sony Corporation, Tokyo, Japan) (mini speech microphone) was attached to the left ear, as shown in Figure 2.1d. The sensitivity of the microphone was -42.0 dB (0 dB = 1 V/1 Pa, 1 kHz). A smartphone (iPhone 6 A1586; Apple, Inc., Cupertino, CA, USA) (smartphone microphone) was held in the left hand while the participants bent their elbow to 90° and their shoulder to 0° and then rotated their arm internally to 45° (Figure 2.1e). Analogue cough sound data were converted into digital signals at a sampling frequency of 100 kHz and stored on a personal computer using the same approach as in cough flow measurement. The digitized cough sound signals were bandpass filtered between 140 Hz to 2000 Hz to minimize artefacts caused by heart sounds and muscle interference. Cough sound signals were converted to absolute values. Subsequently, the absolute values of the waveform of cough sounds were smoothed using a 20 -ms time window to extract the envelopes [42]. The *CPSL* value was calculated from the maximal value of the cough sound data obtained under different experimental conditions using LabChart version 8 software (Figure 2.2b,d,e).

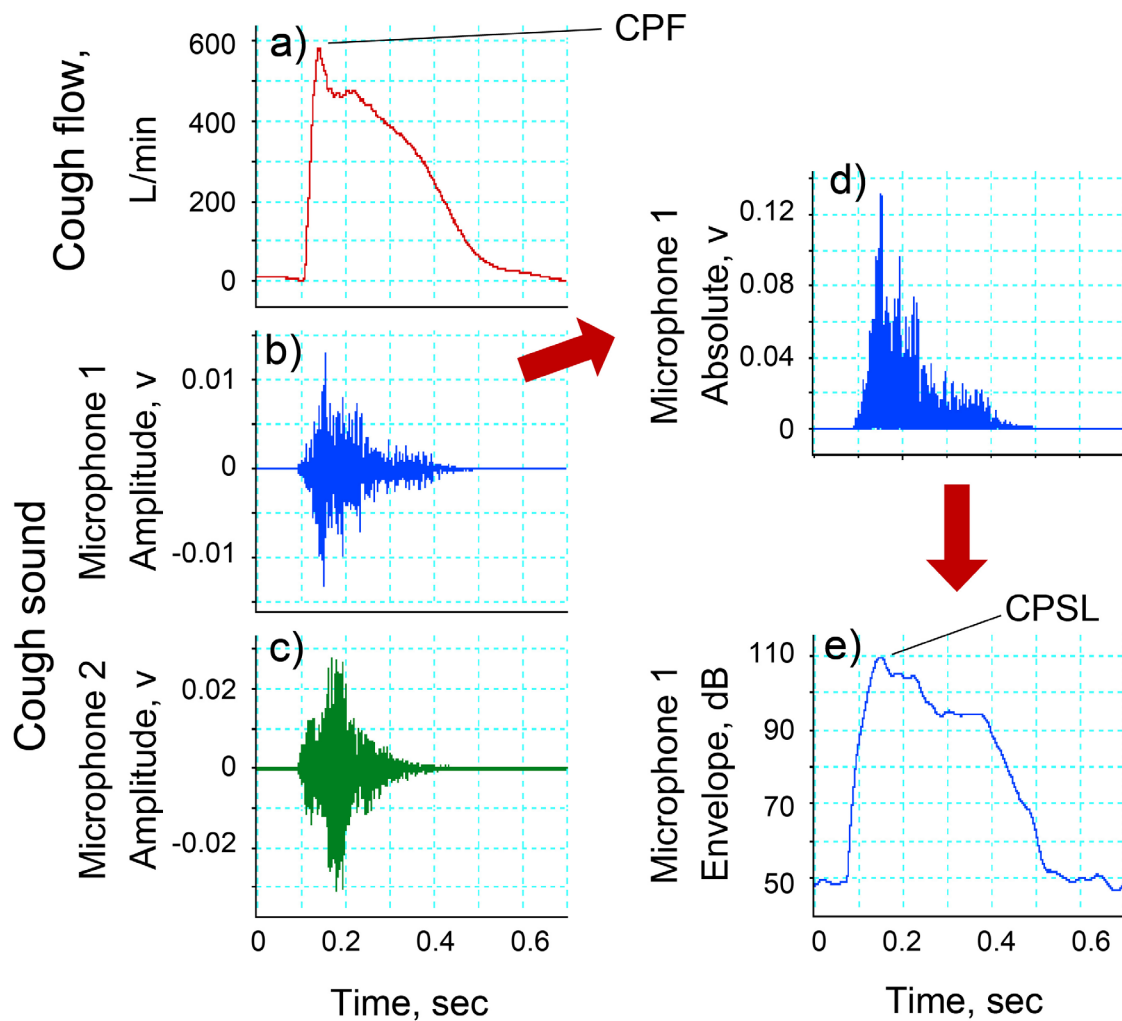


Figure 2.2 Examples of cough flow and cough sounds measured by microphones 1 and 2. (a) Experimental data of cough flow signals in experiment 1. *CPF*, cough peak flow. (b) Experimental data of cough sound signals measured by microphone 1 attached to the flow sensor in experiment 1. (c) Experimental data of cough sound signals measured by microphone 2 fixed to the microphone stand in experiment 1. (d) Absolute values of cough sound measured by microphone 1. (e) Envelope of cough sound signals calculated from the absolute cough sound values measured by microphone 1. *CPSL* is defined as the maximum value of the envelope.

Experimental Protocols

Experiments 1 and 2

Participants' voluntary coughs were measured under three different conditions: five times with maximal effort from a maximal inspiratory level; five times with maximal effort from a resting inspiratory level; and five times with slight effort from a resting inspiratory level. Thus, a total of 15 cough flows and cough sounds per participant were measured simultaneously. Therefore, the total cough sample size was 495.

The participants were provided with sufficient instructions regarding the cough methods and had practice coughing sessions before the experiment. During the practice and experimental sessions, visual feedback of the flow-volume loop associated with inspiration and cough was provided in real time on a personal computer screen. In the measurement of slight cough, a physical therapist confirmed that minimum effort cough was performed with proper cough sounds. The participants were allowed enough rest time between each trial to reduce the effects of fatigue.

Experiment 3

Maximal voluntary coughing was performed three times after providing sufficient instructions to the participants regarding the cough method. The participants had enough rest between each trial to reduce the effects of fatigue. *CPF* and *CPSL* were determined as the maximum value of each set of measured values.

Statistical Analysis

The Spearman's rank correlation coefficient analysis was used to analyse the relationship between *CPS* and *CPF* and the estimation accuracy of *CPS*. In addition, the absolute error was calculated from *CPS* and *CPF*. The absolute reliability was investigated using the Bland–Altman analysis method to detect systematic bias, such as fixed and proportional bias. The Friedman test was used to compare the absolute error of different distances from the sound source to the microphone, and different microphone types. The Mann–Whitney U test was used to compare the absolute error between the gender groups. The Bonferroni test was used for post hoc analysis.

All statistical tests in this paper assumed a significance level of 0.05 and analyses were performed using G*power (version 3.1.9.2; University Kiel, Kiel, Germany) and SPSS Statistics (version 24.0; IBM, Chicago, IL, USA).

2.4 Results

Relationships between *CPF* and *CPSL* and Verification of the Microphone Installation Method

Figure 2.2 shows examples of cough flow and cough sounds measured by microphones 1 and 2 (Figure 2.1a). Although the cough flow and cough sounds were measured using different methods, both responded to the initiation of the participant cough almost simultaneously. Figure 2.3a shows the relationship between *CPF* and *CPSL* measured by microphone 1 attached to the flow sensor. The coefficients of Equation (2.1), determined by the Levenberg-Marquardt

method, are as follows: $\alpha = 5.67$ (95% confidence interval (CI): 4.557 to 6.784) and $\beta = 0.044$ (95% CI: 0.042 to 0.046); the determination coefficient was 0.843. Therefore, the following estimation formula could be derived from $CPSL$ measured by microphone 1:

$$CPF = 5.67(e^{0.044CPSL} - 1). \quad (2.7)$$

Figure 2.3b shows the relationship between CPF and CPS , which confirmed a significant positive correlation ($r = 0.920$; $P < 0.001$; power, 100%).

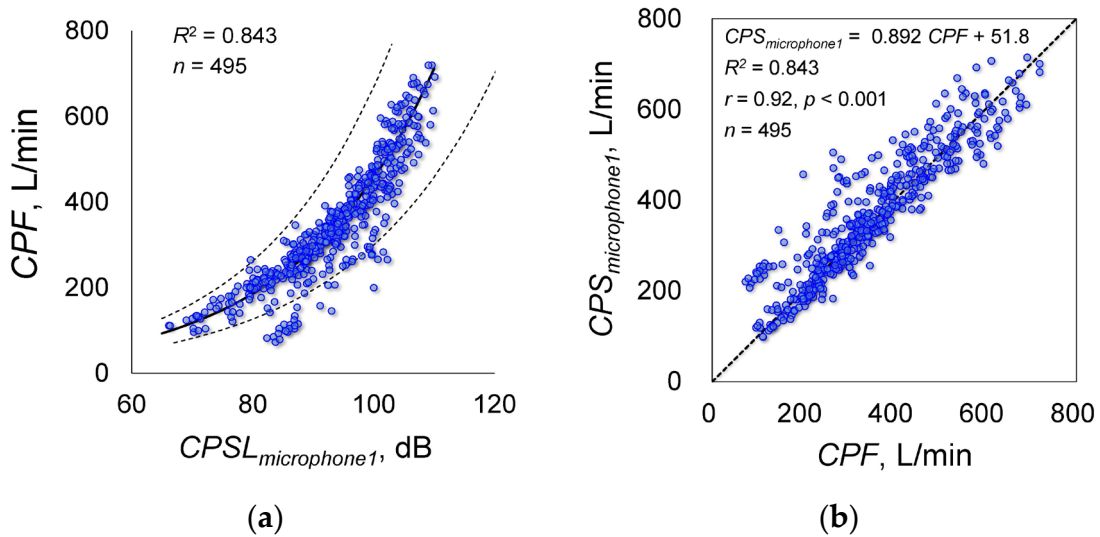


Figure 2.3 Estimation accuracy of Equation (2.7) calculated from the experimental data measured by microphone 1 attached to the flow sensor. **(a)** Relationship of CPF and $CPSL_{microphone1}$. The solid lines represent the regression curves derived by fitting the coefficients in the proposed model using the Levenberg-Marquardt method based on CPF and $CPSL_{microphone1}$. The dotted lines represent 95% confidence bands. CPF , cough peak flow; $CPSL_{microphone1}$, cough peak sound pressure level by microphone 1. **(b)** Relationship between CPF and $CPS_{microphone1}$. $CPS_{microphone1}$, estimated cough peak flow calculated from $CPSL_{microphone1}$.

In case of the experimental data measured by microphone 2 fixed to the microphone stand (Figure 2.1a), the Levenberg-Marquardt method showed that the coefficients obtained are as follows: $\alpha = 38.731$ (95% CI: 24.071 to 53.391), $\beta = 0.026$ (95% CI: 0.023 to 0.030); the determination coefficient was 0.455. The Spearman's rank correlation coefficient analysis showed a significant positive correlation between *CPF* and *CPS* ($r = 0.699$; $P < 0.001$; power, 100%). The Bland-Altman plot of *CPF* and *CPS* did not show fixed bias but did show proportional bias ($r = -0.453$; $P < 0.001$; power, 100%). Thus, the estimation accuracy of Equation (2.7) calculated from the experimental data measured by microphone 1 was higher than that measured by microphone 2.

Effects of Microphone Distance from the Sound Source on Estimation Accuracy

The cough sounds were measured by five microphones in the same model as experiment 1. These microphones were installed at 20 cm, 30 cm, 40 cm, 50 cm and 60 cm from the point of face mask contact with the face of the participant (Figure 2.1b). Figure 2.4 shows the results of the experimental data for each distance and the correlation analysis between *CPF* and *CPS*. The determination coefficients were 0.864 for 20 cm, 0.841 for 30 cm, 0.619 for 40 cm, 0.556 for 50 cm and 0.554 for 60 cm. The correlation coefficients were 0.903 ($P < 0.001$; power, 100%) for 20 cm, 0.909 ($P < 0.001$; power, 100%) for 30 cm, 0.775 ($P < 0.001$; power, 100%) for 40 cm, 0.76 ($P < 0.001$; power, 100%) for 50 cm and 0.747 ($P < 0.001$; power, 100%) for 60 cm. The absolute errors were 40.5 ± 26.7 L/min for 20 cm, 41.3 ± 30.6 L/min for 30 cm, 64.9 ± 46.2 L/min for 40 cm, 70.7 ± 49.0 L/min for 50

cm and 72.0 ± 47.5 L/min for 60 cm. Figure 2.5 shows the results of the Friedman and Bonferroni tests between the absolute error of each distance. The Friedman test showed that there was a significant difference among the absolute errors ($P < 0.001$). The Bonferroni test showed that the absolute errors were significantly lower for 20 cm and 30 cm than for 40 cm, 50 cm and 60 cm ($P < 0.001$).

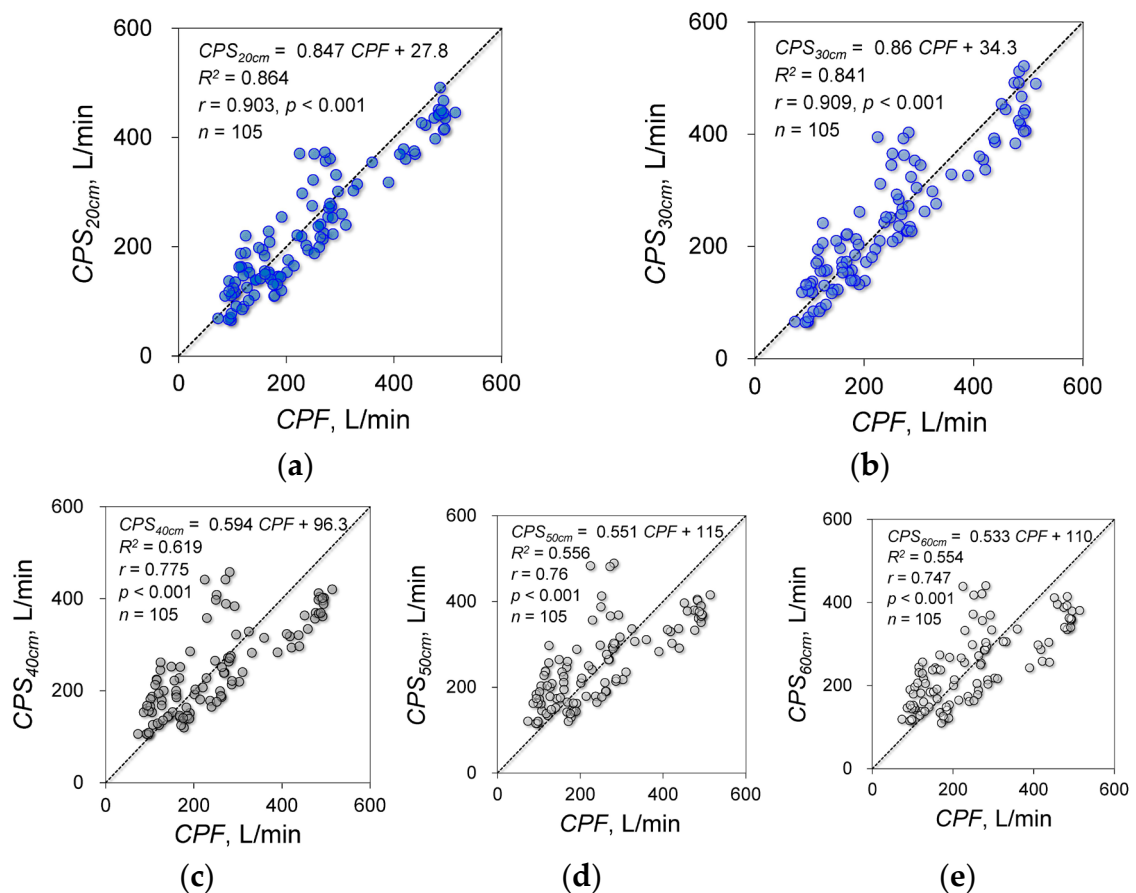


Figure 2.4 Estimation accuracy in each measurement condition. (a–e): Scatter plots of the measured data and the regression results of the proposed model: $CPSL_{20\text{ cm to }60\text{ cm}}$, cough peak sound pressure level measured by each microphone installed 20 cm, 30 cm, 40 cm, 50 cm and 60 cm from the point of face mask contact with the face; $CPS_{20\text{ cm to }60\text{ cm}}$, estimated cough peak flow calculated by $CPSL_{20\text{ cm to }60\text{ cm}}$. Solid lines represent regression lines derived from CPF and CPSL. The variation around the identity line is visibly reduced in graphs (a, b).

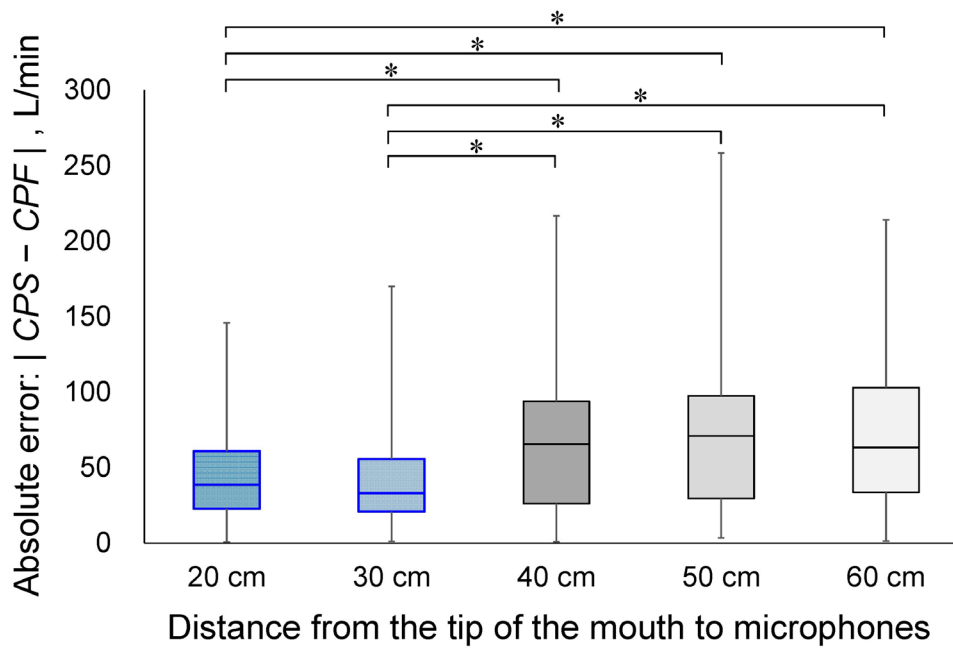


Figure 2.5 Comparison of the absolute error between each measurement condition. *CPF*, cough peak flow; *CPS*, estimated cough peak flow; * $P < 0.001$.

Effects of Microphone Type on Estimation Accuracy

A total of 33 young healthy participants were included in experiment 3. Based on the measurement of cough sounds using the in-ear microphone, the mini speech microphone and the smartphone microphone, CPS_{in-ear} , $CPS_{mini-speech}$ and $CPS_{smartphone}$ were estimated, respectively.

Figure 2.6 shows the results of the experimental data measured by each microphone and the correlation and regression analysis results between *CPF* and each *CPS*. The determination coefficients between *CPF* and each *CPS* estimated by the in-ear, mini speech and smartphone microphones were 0.763, 0.782 and

0.641, respectively. Significant positive correlations were found between CPF and each CPS (in-ear microphone: $r = 0.895$; $P < 0.001$; power, 100%, mini speech microphone: $r = 0.879$; $P < 0.001$; power, 100%, smartphone microphone: $r = 0.795$; $P < 0.001$; power, 99.9%). The absolute errors were 27.3 ± 22.6 L/min, 29.9 ± 27.4 L/min and 38.8 ± 35.7 L/min for the in-ear, mini speech and smartphone microphones. The Friedman test showed that there were no significant differences among the absolute errors ($P = 0.157$).

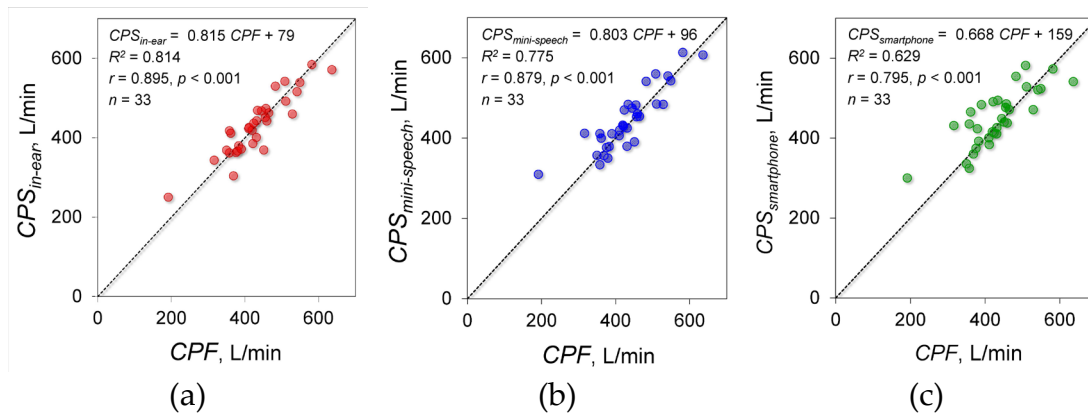


Figure 2.6 The results of experiment 3. CPF , cough peak flow; CPS_{in-ear} , estimated CPF calculated from cough sound measured using the in-ear microphone; $CPS_{mini-speech}$, estimated CPF calculated from cough sound measured using the mini speech microphone; $CPS_{smartphone}$, estimated CPF calculated from cough sound measured using the smartphone microphone. (a) Relationship between CPF and CPS_{in-ear} . (b) Relationship between CPF and $CPS_{mini-speech}$. (c) Relationship between CPF and $CPS_{smartphone}$.

Effects of Participant's Height on Estimation Accuracy

To consider the effect of height on the estimation accuracy of CPF , height parameters were introduced in the proposed model, such as Equation (2.2). The coefficients a_1 , a_2 and β were determined by the Levenberg-Marquardt method

using the measured data of experiment 1 measured by microphone 1 attached to the flow sensor. This model yielded a determination coefficient of 0.843. The determined coefficients were as follows: $a_1 = -0.001$ (95% CI: -0.012 to 0.01), $a_2 = 5.767$ (95% CI: 3.946 to 7.588) and $\beta = 0.042$ (95% CI, 0.04 to 0.044).

Effects of Gender on Estimation Accuracy

To consider the effect of gender on the estimation accuracy of *CPF*, the participants were divided into male and female groups and the coefficients of the proposed model, such as Equation (1), were determined for the respective groups. The coefficient α values were 8.3 ± 5.8 for the male group and 7.5 ± 5.4 for the female group. The Mann-Whitney U test showed no significant difference in the coefficient α values between the male and female groups ($P = 0.653$). The coefficient β values 0.049 ± 0.027 for the male group and 0.044 ± 0.01 for the female group. The Mann-Whitney U test showed no significant difference in the coefficient β values between the male and the female groups ($P = 0.506$).

Comparison between the Proposed Model and Polynomial Functions

To demonstrate the efficacy of the proposed model, its estimation accuracy was compared with the polynomial functions without intercepts, such as Equations (2.3)–(2.6). The coefficients $\alpha_{3 \text{ to } 12}$ were determined by the Levenberg-Marquardt method in the same manner as in the proposed model. Table 2.2 shows the determined parameters and statistical analysis results. The 95% CIs of all

coefficients in Equation (2.6) include 0, which indicates that the fourth-order polynomial function is redundant to estimate cough peak flow. Based on these results, the following analysis used our proposed model of Equation (2.1) and Equations (2.3)–(2.5). The absolute errors between *CPF* and *CPS* were 40.0 ± 41.8 L/min in the proposed model, 89.7 ± 65.2 L/min in Equation (2.3), 43.7 ± 39.9 L/min in Equation (2.4) and 98 ± 62.8 L/min in Equation (2.5). The Friedman test showed that there was a significant difference among the absolute errors ($P < 0.001$). The Bonferroni test showed that the absolute error was significantly lower in the proposed model and Equation (2.4) than in Equations (2.3) and (2.5) ($P < 0.001$). In addition, Figure 2.7 shows the corresponding Bland-Altman plot of the proposed model and Equation (2.4). The proposed model did not show fixed bias and proportional bias. However, Equations (2.4) did not show fixed bias but did show proportional bias ($r = -0.343$, $P < 0.001$).

Table 2.2 Relationship between cough peak flow and cough peak sound pressure level using Equations (2.3)–(2.4).

| Estimation Equation | Coefficient | Estimated Value | Standard Error | 95% CI | | Determination Coefficient |
|---------------------|---------------|-----------------|----------------|---------|--------|---------------------------|
| | | | | Lower | Upper | |
| Equation (2.3) | α_3 | 3.819 | 0.053 | 3.714 | 3.923 | 0.373 |
| Equation (2.4) | α_4 | 0.117 | 0.003 | 0.111 | 0.124 | 0.822 |
| | α_5 | -7.288 | 0.317 | -7.910 | -6.665 | |
| Equation (2.5) | α_6 | 0.002 | 0.000 | 0.002 | 0.003 | 0.843 |
| | α_7 | -0.326 | 0.054 | -0.431 | -0.220 | |
| | α_8 | 13.013 | 2.249 | 8.132 | 17.895 | |
| Equation (2.6) | α_9 | 0.019 | 0.000 | -0.015 | 0.052 | 0.844 |
| | α_{10} | -0.005 | 0.007 | -0.019 | 0.008 | |
| | α_{11} | 0.355 | 0.617 | -0.858 | 1.567 | |
| | α_{12} | -7.198 | 18.431 | -43.412 | 29.02 | |

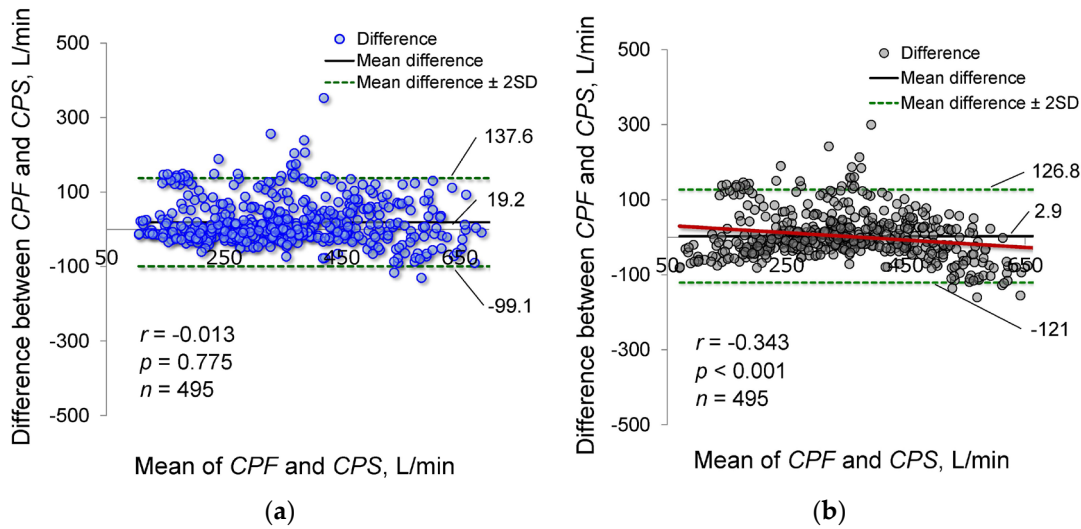


Figure 2.7 Bland-Altman plot of the measured and estimated cough peak flow. *CPF*, cough peak flow; *CPS*, estimated cough peak flow. **(a)** *CPS* estimated using our proposed model of Equation (2.1). **(b)** *CPS* estimated using Equation (2.4). Blue and black dots represent the difference between *CPF* and *CPS*. Bold black solid lines represent the mean difference between *CPF* and *CPS*. Green dotted lines represent the mean difference \pm 2 standard deviation bands. Red lines represent the approximate straight line of the difference between *CPF* and *CPS* and the mean of *CPF* and *CPS*.

2.5 Discussion

To the best of our knowledge, this is the first study to develop a method for estimating cough strength via cough sounds using a model represented by an exponential equation. Analysis of the results of experiment 1 demonstrated that *CPS* calculated from the cough sound measured using microphone 1 attached to a flow sensor is estimated to have high accuracy. Moreover, the *CPF* estimation accuracy using microphone 1 is significantly higher than that using microphone 2 fixed to the microphone stand. This is because microphone 1 was attached to the flow sensor, which maintained a fixed distance from the vocal cords but the

distance between microphone 2, which was attached to the microphone stand and the vocal cords could be changed by inspiratory and/or coughing-induced body motion. The decrease in the sound level L_p can be calculated by the distance from the sound source r_1, r_2 using the following equation:

$$L_p = 20 \log \left(\frac{r_2}{r_1} \right). \quad (1.8)$$

The fact that the sound pressure level decreases with distance from the sound source indicates that body motion may be a cause of artefacts and, therefore, reduces estimation accuracy. Thus, to improve estimation accuracy, microphones should be installed on the body so that the microphones can maintain a constant distance from the sound source. Based on the results, we selected three types of wearable microphones (the in-ear microphone, the mini speech microphone and the smartphone microphone).

In experiment 2, we found that the distance between the mouth, as a sound source and the microphone needs to be less than 30 cm. Sound propagation in a room is a combination of direct and reflected sound waves from surfaces and boundaries in the room [61]. In addition, the sound attenuates with increasing distance from the sound source, as shown in Equation (2.8). When the microphone is set at a distance more than 30 cm from the mouth, the measured cough sounds may be influenced by sounds reflected from the walls and/or sound attenuation.

In experiment 3, we used three types of microphones (i.e., an in-ear microphone, a mini speech microphone and a smartphone microphone) to measure cough sounds. The strongest correlation between CPF and CPS was estimated using data obtained from the in-ear microphone. Thus, these

microphones could be introduced as simple and wearable cough strength measurement devices.

In the respiratory function test, participant height is generally used to determine the normal level of respiratory function [62,63] and a relationship between *CPF* and height has been reported [64]. Based on these previous studies, we hypothesized that height affects *CPS*; however, in Equation (2), in which the coefficient α of Equation (2.1) was replaced by a linear function of height, the 95% CI of the multiplication coefficient α_1 onto the height ranged from -0.112 to 0.02 , including 0 . This result indicates that height has a minimal effect on the *CPF* estimation accuracy.

Previous studies have also suggested that normal respiratory function levels vary according to gender [62,63] and the *CPF* of male participants has been shown to be significantly higher than that of female participants [64]. Therefore, we hypothesized that gender can affect the coefficients in the estimation equation; however, no significant difference in estimation accuracy was found between male and female participants. This result demonstrates that gender also has a minimal effect on the estimation accuracy when adopting the proposed model, represented by Equation (2.1).

We verified the prediction equation using first- to fourth-order polynomial functions. Several previous studies have reported that the relationship between air flow and breath sound amplitude is linear under high flow rate conditions [5,6]. It has also been reported that the sound amplitude during inspiration is proportional to the square of the air flow at the mouth [7,65]. Moreover, it was shown that the flow profile of inhalations can be estimated based on the logarithmic relationship between the acoustic envelope of

the inhalation sound and the flow volume [59]. In contrast, a strong linear correlation between cough sound and cough flow has also been reported [66]. Our study revealed a nonlinear relationship between cough sound and cough flow. Thus, cough sounds were proportional to the square of the cough flow; however, a proportional bias was found in the second-order polynomial function, as observed for Equation (2.4). The effectiveness of the proposed model, represented by the exponential function, such as Equation (2.1), was verified by the fact that it successfully eliminated this systematic bias.

A major limitation of this study is that we did not fully consider the effect of age and disease, since the study participants were young Japanese healthy volunteers. In the respiratory function test, participant age is generally used to determine the normal level of respiratory function [62,63] and a relationship between *CPF* and age has been reported [64]. Also, the body weight or BMI of subjects may have impact on accuracy of estimated *CPF*. In addition, because the model was derived empirically in this study, its physiological and physical aspects must be addressed. Moreover, because the experimental results showed that maintaining a constant distance between the mouth, as a source of sound and the microphone is key to improving estimation accuracy, it will be necessary to develop a more suitable type of microphone. A wearable microphone, such as a piezoelectric bone conduction microphone, is one such candidate for application as the base technique.

2.6 Concluding Remarks

This paper has proposed a nonlinear model for predicting the cough strength in young Japanese youth via cough sounds. Future studies should verify whether age, body weight and BMI influence the accuracy of the prediction model. If large variabilities in age, body weight and BMI that are to be expected in patients in the world are included and considered in the analysis, a practical device for assessing cough strength may be developed by employing the proposed model. The effects of age, body weight and BMI, the most suitable type of microphones and the physiological and physical explanations of the proposed model will be investigated in future work.

Chapter 3

Effects of Microphone Type on Cough Strength Estimation

3.1 Introduction

Cough is an important protective mechanism that causes the central airways to be cleared of foreign materials and excess secretions [67]. Objective analysis of cough may provide a noninvasive method to identify aspiration risk [68,69], and it has been proposed that researchers should focus on techniques to improve coughing dysfunction, rather than develop new antibiotics, to decrease mortality due to aspiration pneumonia in the elderly [35]. To prevent aspiration pneumonia, the evaluation of the ability to cough is therefore as important as that of swallowing function.

The assessment of cough effectiveness includes measurements of CPF [23,24,29-31,70]. Bach and Saporito concluded that the ability to generate CPF of at least 160 L/min is necessary for a successful extubation or tracheostomy tube

decannulation because an intercurrent upper respiratory tract infection and the inability to clear airway secretions trigger acute respiratory failure [29,30]. Patients that can generate CPF of more than 270 L/min have little risk of developing respiratory failure during upper respiratory tract infections [31].

In the conventional CPF measurement method, a face mask is attached to a spirometer or a peak flow meter to prevent infection, and subjects are required to cough voluntarily. However, the disadvantage of this method is that the measured CPF changes depending on the type of face masks or bacterial filters. In addition, the mask, which is firmly attached to the patient's face to prevent air leakage, makes it difficult for the subject to perform natural and voluntary cough.

Therefore, this study has aimed to develop a simple evaluation system to assess the cough ability through cough sound without any face mask or bacterial filter. Several previous studies proposed methods to monitor cough frequency using a microphone in patients with asthma [38,39,54-58,71], but not for the cough ability. If the assessment of the cough ability through cough sound is feasible, it can be applied to patients in whom measurements of cough peak expiratory flow using the current method are difficult. In our previous studies, the relationship between CPF and the peak cough sound pressure level (CPSL) was assumed to be an exponential function. Using the proposed method, predicted cough peak expiratory flow CPS was calculated considering the effect of the subject height or gender [72]. However, the effects of the type of microphone on measured cough sounds and predicting CPS has not yet been verified. Therefore, this study aims to verify the effects of the type of microphone on CPS to develop a novel evaluation system.

3.2 Experimental Methods

This study was conducted in accordance with the amended declaration of Helsinki. The Hiroshima Cosmopolitan University Institutional Review Board (No. 2015031) approved the protocol, and written informed consent was obtained from all participants.

Participants

A total of 25 young healthy subjects with no history of lung disease participated in the experiments. The mean \pm standard deviation age of subjects was 21.0 ± 0.2 years (range: 21 - 22 years), the mean height of subjects was 165.5 ± 8.7 cm, and the mean weight of subjects was 61.1 ± 12.4 kg. The absence of pulmonary disease was ascertained in advance by inquiry and pulmonary function test.

Measurement method of cough flows

Measurement of cough was carried out in a sitting position. To measure cough flow, participants wore a face mask with a flow sensor (Mobile aero monitor AE-100i; Minato Medical Science Co., Ltd., Osaka, Japan) attached. The maximum value of the obtained cough flow data was defined as CPF. The measurement range of the flow sensor was 0 - 840 L/min, and the measurement accuracy was within 3% of the indicated value.

Measurement method of cough sounds

Figure 3.1 shows the cough sound measurement method. Cough sound was

measured using three types of microphones. To measure cough sound through in-ear from the right external auditory canal, an electret condenser microphone (ECM-TL3; Sony Corporation, Japan) (in-ear microphone) was attached to the right ear canal (Figure 1a). The sensitivity of the microphone was -35.0 dB (0 dB \pm 1 V/1 Pa, 1 kHz). A headset mini speech microphone (ECM-322BMP; Sony Corporation, Japan) (mini speech microphone) was attached to the left ear (Figure 3.1b). The sensitivity of the microphone was -42.0 dB (0 dB \pm 1 V/1 Pa, 1 kHz). The cough sound signal was digitized using a 16 bit analog-to-digital converter (PowerLab16/35, ADInstruments, Inc., Dunedin, New Zealand) at a 100 kHz sampling rate set by an analysis software (LabChart version 8, ADInstruments, Inc.). CPSL was calculated from the maximal value of the cough sound pressure level obtained from the different types of microphone. The smartphone (iphone6 A1586; Apple Inc., United States of America) (smartphone microphone) was held in the left hand while flexing the subject's elbow to 90° and the shoulder to 0° , and then internally rotating it to 45° (Figure 3.1c).



Figure 3.1 Types of microphones and measurement position. (a) In-ear microphone. (b) Mini speech microphone. (c) Smartphone microphone.

To check the variation in the distance from the sound source to each microphone between subjects, we measured the distance from the edge of the lip to each microphone. In the case of the in-ear microphone, the distance from the microphone to the thyroid cartilage was measured.

Protocol

After giving sufficient cough method instruction to the subjects, maximal voluntary coughing was performed three times. Subjects had enough rest between each trial to reduce fatigue effects. *CPF* and *CPSL* were determined as the maximum value of each set of measured values.

Analysis

The rank correlation coefficient of Spearman evaluates the relationship of the distance from the sound source to each microphone and the height. The relationship between *CPF* and *CPSL* was assumed to be an exponential function [72] as in the following equation:

$$CPF = \alpha \cdot (exp^{\beta \cdot CPSL} - 1) \quad (3.1)$$

where α and β are constants. To establish a prediction formula for predicted *CPF* (*CPS*), the coefficients a_1 and a_2 in (1) were determined by non-linear regression analysis (Levenberg-Marquardt method) using *CPF* and *CPSL* obtained from each microphone. To verify the effect of the height (h) on *CPS*, the expression in (2) was proposed by including the height variable in (1) as follows:

$$CPF = (\alpha_1 \cdot h + \alpha_2) \cdot (exp^{\beta_{(3.2)} \cdot CPSL} - 1) \quad (3.2)$$

where α_1 , α_2 , and $\beta_{(3.2)}$ are constants. To verify the prediction accuracy of *CPS*, the relationship between *CPS* and *CPF* was evaluated using the Spearman's rank correlation coefficient and regression analysis. In addition, the relative error was calculated from *CPS* and *CPF*. Absolute reliability was investigated using the Bland-Altman analysis method to detect systematic errors, such as the fixed error and proportional error [73]. The Friedman test was used to compare the relative error between different microphone types. *CPSL* and *CPS* obtained from the in-ear microphone were, respectively expressed as $CPSL_{in-ear}$ and CPS_{in-ear} , those obtained from the mini speech microphone were expressed as $CPSL_{mini-speech}$ and $CPS_{mini-speech}$, and those obtained from the smartphone microphone were expressed as $CPSL_{smartphone}$ and $CPS_{smartphone}$.

All statistical calculations were carried out using the IBM SPSS Statistics

24 for Windows. A value of $P < 0.05$ was considered to be statistically significant.

3.3 Results

Relationship between distance from sound source to each microphone and height

No significant correlation was found between the distance from the thyroid cartilage to the in-ear microphone, as well as the height ($r = 0.177$, $P = 0.398$). No significant correlation was found between the distance from the edge of the lip to the mini speech microphone, as well as the height ($r = -0.046$, $P = 0.827$). A positive significant correlation was found between the distance from the lip to the smartphone microphone, as well as the height ($r = 0.452$, $P = 0.023$).

Non-linear regression

Figure 3.2 and Table 3.1 show the results of the non-linear regression analysis of the experimental data measured using each microphone. The determination coefficients of the in-ear microphone by Equations (3.1) or (3.2) were: $R^2 = 0.827$ and $R^2 = 0.829$. The determination coefficients of the mini speech microphone by Equations (3.1) or (3.2) were $R^2 = 0.835$ and $R^2 = 0.837$. The determination coefficients of the smartphone microphone by Equations (3.1) or (3.2) were $R^2 = 0.713$ and $R^2 = 0.737$. In all cases, the determination coefficients were slightly higher in Equation (3.2) with respect to the height variable.

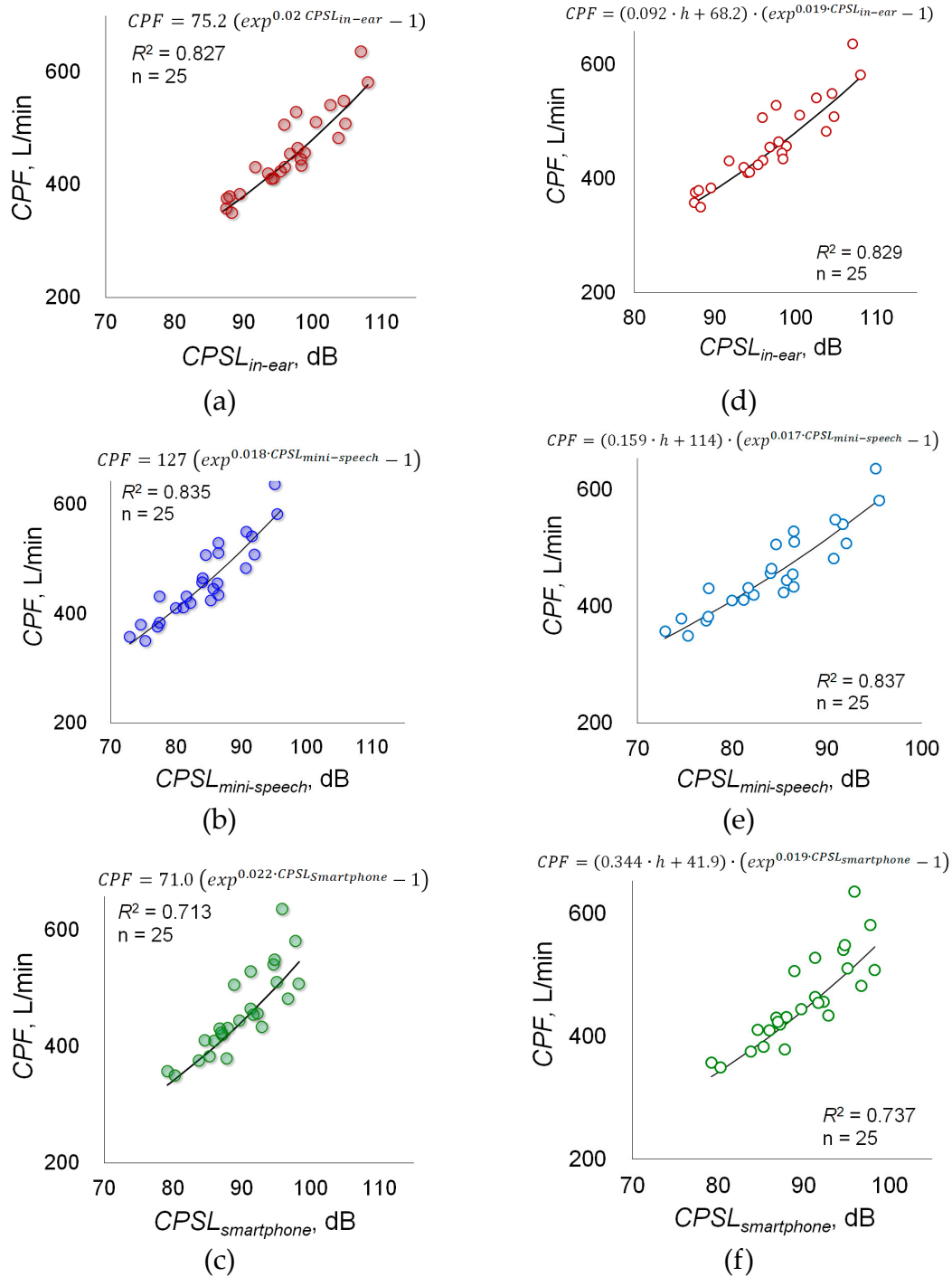


Figure 3.2 Results of non-linear regression analysis. (a) In-ear microphone. Non-linear regression using Equation (3.1). (b) Mini speech microphone. Non-linear regression using Equation (3.1). (c) Smartphone microphone. Non-linear regression using Equation (3.1). (d) In-ear microphone. Non-linear regression using Equation (3.2). (e) Mini speech microphone. Non-linear regression using Equation (3.2). (f) Smartphone microphone. Non-linear regression using Equation (3.2).

Table 3.1 Results of non-linear regression.

| Type of microphone | Coefficient | Estimated value | 95% CI | | Determination Coefficient |
|------------------------|-----------------|-----------------|--------|-------|---------------------------|
| | | | Lower | Lower | |
| In-ear microphone | α | 75.2 | 25.0 | 125.5 | 0.827 |
| | $\beta_{(3.1)}$ | 0.020 | 0.014 | 0.026 | |
| | α_1 | 0.092 | -0.309 | 0.493 | 0.829 |
| | α_2 | 68.2 | 11.0 | 125.6 | |
| | $\beta_{(3.2)}$ | 0.019 | 0.012 | 0.026 | |
| Mini speech microphone | α | 127.2 | 44.1 | 210.3 | 0.835 |
| | $\beta_{(3.1)}$ | 0.018 | 0.012 | 0.024 | |
| | α_1 | 0.159 | -0.507 | 0.826 | 0.837 |
| | α_2 | 114.6 | 18.9 | 210.3 | |
| | $\beta_{(3.2)}$ | 0.017 | 0.010 | 0.024 | |
| Smartphone microphone | α | 71.0 | 3.4 | 138.6 | 0.713 |
| | $\beta_{(3.1)}$ | 0.022 | 0.013 | 0.031 | |
| | α_1 | 0.344 | -0.415 | 1.102 | 0.737 |
| | α_2 | 41.9 | -33.0 | 116.8 | |
| | $\beta_{(3.2)}$ | 0.019 | 0.009 | 0.030 | |

Accuracy of each predicted equation

Figure 3.3 and Table 3.2 show the results of the correlation and regression analysis between *CPS* and *CPF*. A strong positive significant correlation was found between each *CPS* and *CPF* ($r = 0.896 - 0.926$). Specifically, the results of *CPS* predicted by Equation (3.2) using the in-ear microphone and the smartphone microphone strongly correlated with *CPF* (Table 3.2). Figure 3.4 shows the results of the Bland-Altman method for assessing the agreement between *CPS* and *CPF*. In all cases, the Bland-Altman analysis showed no systematic error between *CPS* and *CPF*.

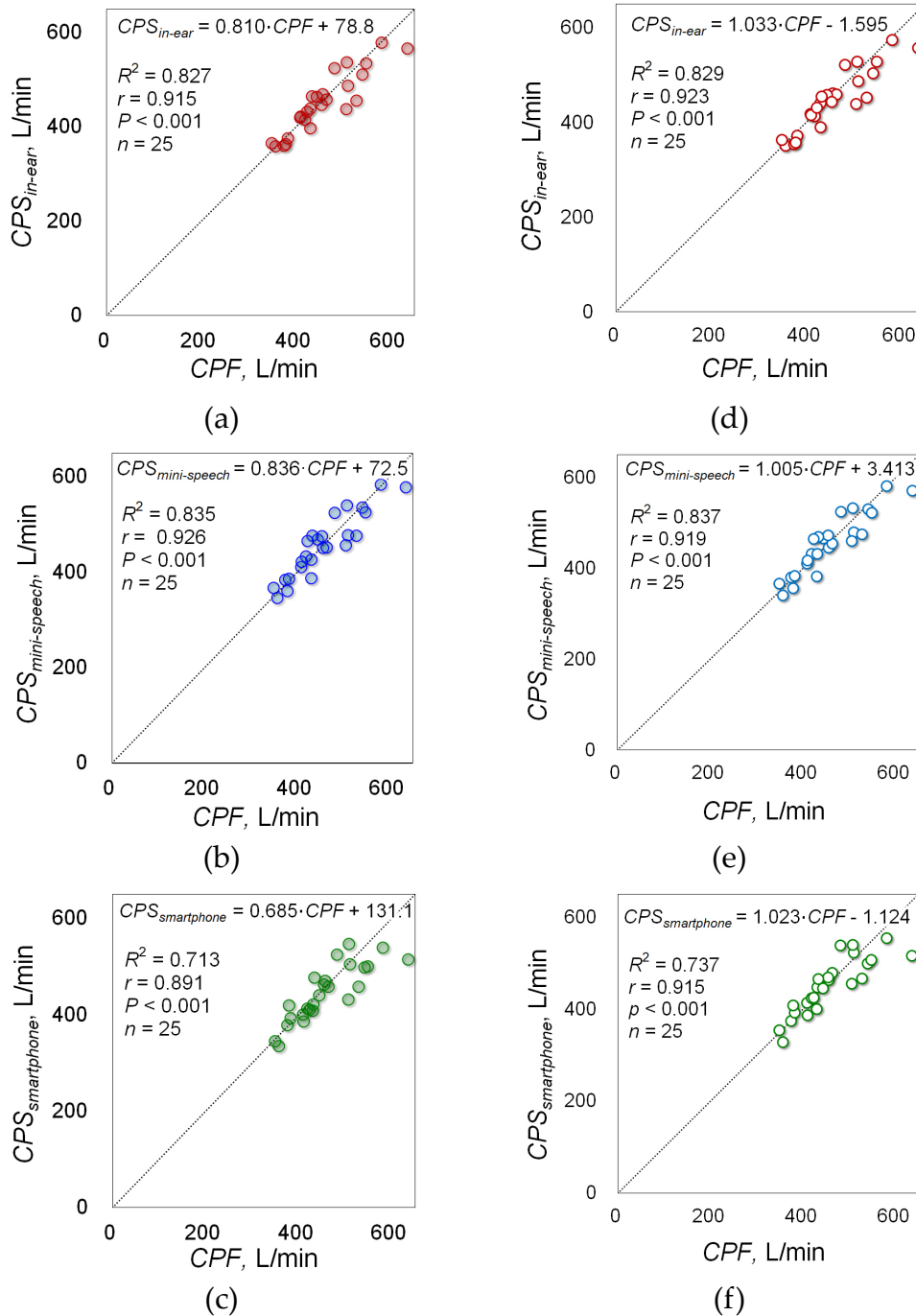


Figure 3.3 Results of the rank correlation coefficient of the Speaman analysis. (a) In-ear microphone. CPS_{in-ear} was calculated using (3.1). (b) Mini speech microphone. $CPS_{mini-speech}$ was calculated using (3.1). (c) Smartphone microphone. $CPS_{smartphone}$ was calculated using (3.1). (d) In-ear microphone. CPS_{in-ear} was calculated using (3.2). (e) Mini speech microphone. $CPS_{mini-speech}$ was calculated using (3.2). (f) Smartphone microphone. $CPS_{Smartphone}$ was calculated using (3.2).

Table 3.2 Results of the rank correlation coefficient of Spearman

| | | Equation (3.1) | | | Equation (3.2) | | |
|-------|-----|----------------|---------------------|--------------------|----------------|---------------------|--------------------|
| | | CPS_{in-ear} | $CPS_{mini-speech}$ | $CPS_{smartphone}$ | CPS_{in-ear} | $CPS_{mini-speech}$ | $CPS_{smartphone}$ |
| CPF | r | 0.915 | 0.926 | 0.891 | 0.923 | 0.919 | 0.915 |
| | P | < 0.001 | < 0.001 | < 0.001 | < 0.001 | < 0.001 | < 0.001 |
| | n | 25 | 25 | 25 | 25 | 25 | 25 |

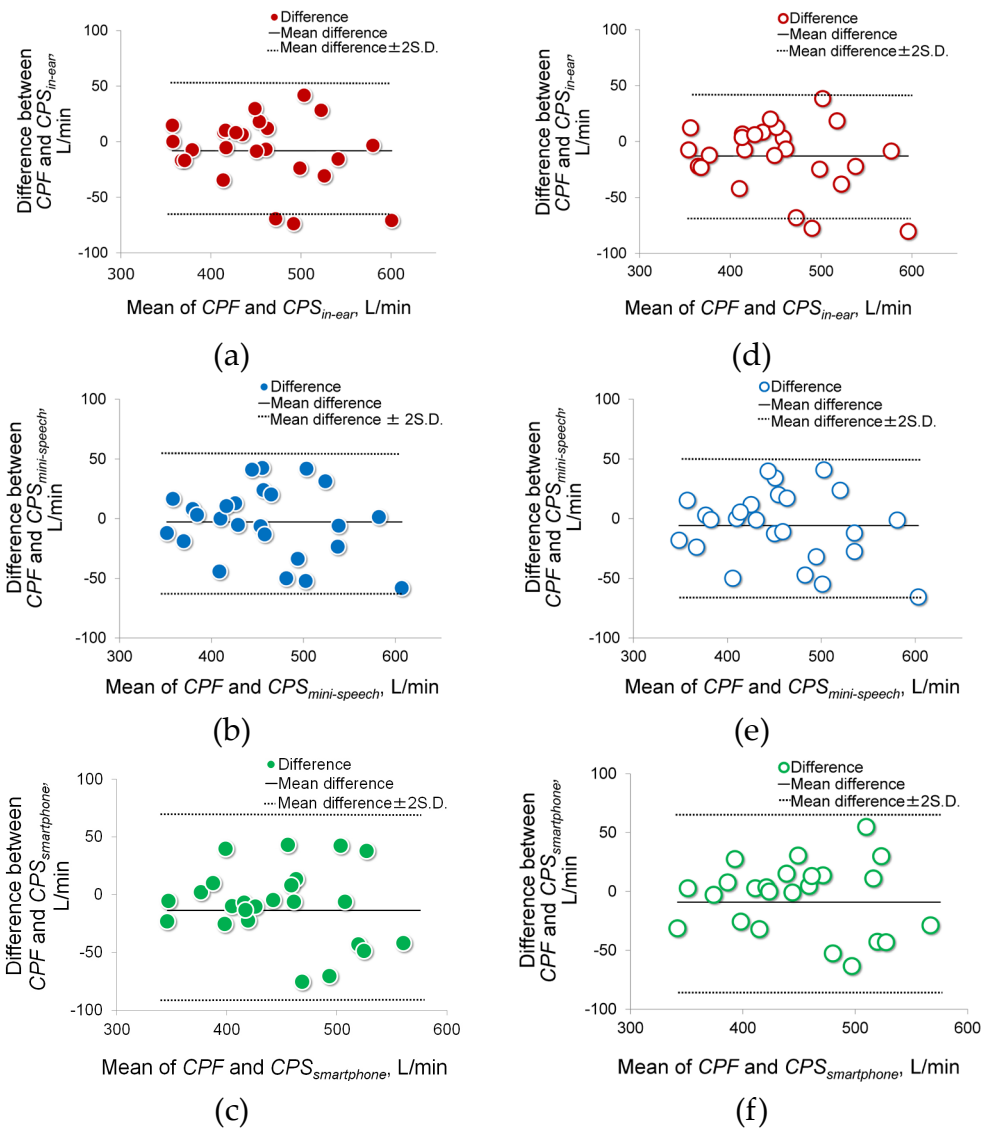


Figure 3.4 Results of the Bland-Altman method for assessing agreement between CPS and CPF . (a) In-ear microphone. (b) Mini speech microphone. (c) Smartphone microphone. (d) In-ear microphone. (e) Mini speech microphone. (f) Smartphone microphone. solid line: mean difference; dashed line: 95% confidence interval of difference.

Comparison results of the relative errors

Figure 3.5 shows results of the comparison of the relative errors between each *CPS* and *CPF*. The relative errors were $4.6 \pm 3.8\%$ by the in-ear microphone in Equation (3.1), $4.9 \pm 3.5\%$ by the mini speech microphone in Equation (3.1), $5.9 \pm 4.9\%$ by the smartphone microphone in Equation (3.1), $4.8 \pm 4.0\%$ by the in-ear microphone in Equation (3.2), $4.8 \pm 3.6\%$ by the mini speech microphone in Equation (3.2), and $5.4 \pm 4.7\%$ by the smartphone microphone in Equation (3.2). The Friedman test showed that there was no significant difference between the relative errors ($P = 0.315$).

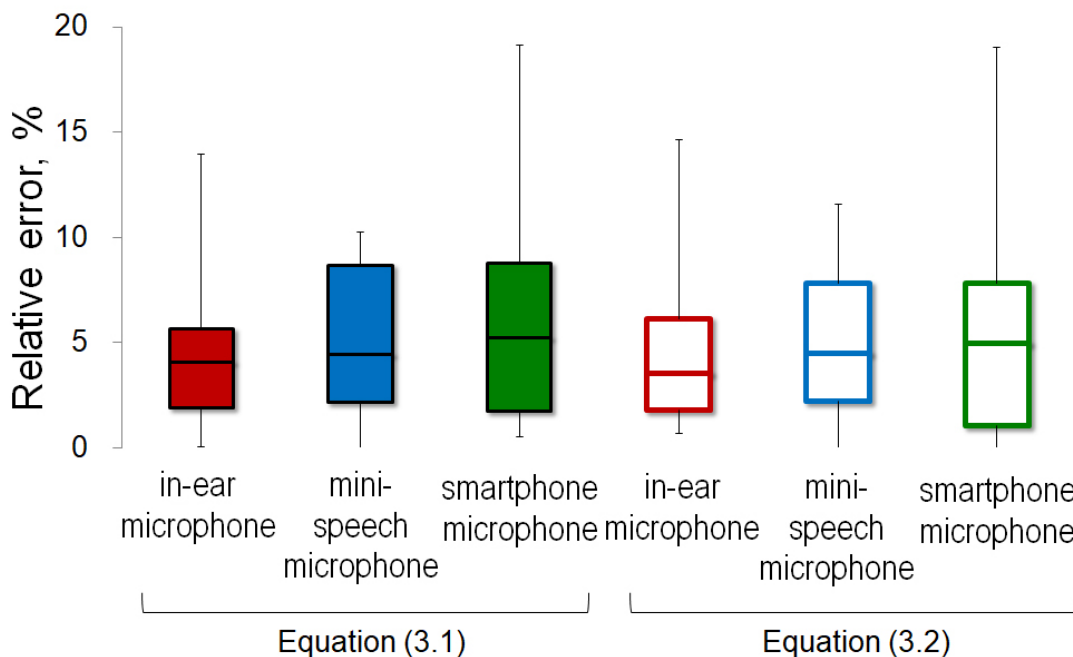


Figure.3.5 Graph comparing the relative errors between different microphone types. Friedman test showed that there was no significant difference between the relative errors ($P = 0.315$).

3.4 Discussion

This study predicted cough peak expiratory flow *CPF* through cough sound based on the knowledge that the respiratory flow rate is related to the breathing sound [5-7], and the relationship between *CPF* and *CPSL* can be expressed by an exponential function [72]. The results of the non-linear regression analysis confirmed high determination coefficients for the mini speech microphone, in-ear microphone, and smartphone microphone. To accurately measure cough sounds, it was necessary to keep a constant distance between the sound source and the microphones without changing the distance by coughing-induced body motion [72]. This is because cough sound decreases with distance from the sound source, and body motion causes artifacts, thereby reducing prediction accuracy. The decrease in sound level L_p can be calculated by the distance from the sound source r_1, r_2 using the following equation:

$$L_p = 20 \log(r_2/r_1) \quad (3.3)$$

The distance from the sound source to the mini speech microphone fixed to the ear was closest and this distance was kept nearly constant, even when coughing-induced body motion occurred; this was the reason the highest determination coefficient was obtained. In the case of the in-ear microphone and the smartphone microphone, the distance from the sound source to these microphones may be changed depending on the subject's height. In particular, results of the correlation analysis showed the relationship between the distance from the lip to the smartphone and the height. Therefore, including the height

variable in (2) improved the accuracy of *CPS* for the conduction microphone and the smartphone microphone.

However, we did not consider the effect of age because all the participants were young volunteers. A relationship between *CPF* and age has been reported [64,74,75]. In addition, previous studies suggested that breath sound can be affected by sound frequency [5-7]. Therefore, the effects of age and cough sound frequency should be investigated in future studies. Moreover, previous studies have proposed methods to extract cough sounds from daily utterances, and clinical application is progressing [18,76,77]. Incorporating these methods to the proposed system may improve accuracy. For clinical application, it is necessary to incorporate such methods into our system to increase prediction accuracy.

3.5 Concluding Remarks

In this study, we proposed a novel cough ability evaluation system through cough sound, and conducted experiments to verify the effects of three types of microphones (in-ear microphone, mini speech microphone, and smartphone microphone) on estimated values of cough peak flow. The results of the non-linear regression analysis confirmed high determination coefficients for the three types of microphones investigated. Furthermore, including the height variable in the prediction equation improved the accuracy of *CPS* for the conduction microphone and the smartphone microphone. However, we did not consider the effects of age and cough sound frequency on *CPS*. These effects

should be investigated in the future. Based on experimental results, we also plan to develop a simple cough ability evaluation system using smartphones that can be used for in-home care.

Chapter 4

A Mobile Cough Strength Evaluation Device Using Cough Sounds

4.1 Introduction

Cough is an important defence mechanism for clearing excess secretions and foreign materials from airways [8,9]. Generally, cough peak flows (CPF) are measured using a spirometer or a peak flow meter to assess cough strength because cough strength reflects the ability to clear secretions from the respiratory tract and indicates the aspiration risk. For example, it is unlikely that someone with a CPF greater than 270 L/min will develop acute respiratory distress [31]. Patients with a CPF greater than 160 L/min can manage ventilatory failure without tracheostomy [29,30]. Dysphagic patients with persistent tracheobronchial aspiration with a CPF less than 242 L/min have a high risk of

developing pulmonary complications [33]. Although previous studies have reported the importance of CPF as a measurement for assessing the ability to expel airway secretions, it requires a face mask and a bacterial filter firmly attached to the patient's mouth, as well as configuration of a complex measurement instrument. This method imposes burdens on both patients and their caregivers and prevents daily CPF measurements in clinical practice.

To solve this problem, our research group developed a CPF estimation method using cough sounds [72,78] by modelling the relationship between the cough sounds and flow rates. The method enabled the estimation of CPF without a face mask or bacterial filter and drastically simplified the measurement instrument configuration because the cough sounds can easily be measured using a microphone. However, the previous method did not fully consider the effect of age, body weight or body mass index (BMI), although relationships between CPF and age and body weight have been reported [64]. In addition, the previous method could not immediately present the estimated result to the patient, as it lacked a user interface. These limitations made it difficult to apply the proposed method in clinical practice.

Therefore, this paper presents a newly proposed CPF estimation model that can account for the relationship between CPFs and cough sounds while considering age, body weight and BMI. In addition, aiming for future applications in the clinic and the home, we also present a user interface incorporating the proposed CPF estimation model for mobile devices that enables cough sound recording, immediate CPF estimation, and estimated CPF history management. Finally, we report the estimation accuracy of the proposed model implemented using a mobile device by performing experiments on young

participants (n = 33) and elderly participants (n = 25).

4.2 Proposed device

In this paper, we propose a CPF estimation model and user interface software for iOS version 11.4 to assess cough strength. The details of the proposed model and the user interface are described in this section.

4.2.1 Model

The proposed model is expressed by the following equation:

$$CPS_{proposed} = (\alpha_{0,(1)} + \alpha_{1,(1)} \cdot age) \cdot (exp^{\beta_{(1)} \cdot CPSL} - 1), \quad (4.1)$$

where $\alpha_{0,(1)}$, $\alpha_{1,(1)}$ and $\beta_{(1)}$ are the parameters predetermined by a non-linear regression analysis (the Levenberg-Marquardt method) using the mean square error between the $CPS_{proposed}$ and the measured CPF as the evaluation function. The $CPSL$ represents the cough peak sound pressure level. This model indicates that the cough peak flow (estimated CPF ($CPS_{proposed}$)) and the $CPSL$ are logarithmically related. The next section describes the preprocessing method used to derive the $CPSL$ from cough sounds, which can be measured using a smartphone.

4.2.2 Measurement protocol and preprocessing for cough sounds

Cough sounds are measured using the microphone built into a smartphone (iPhone 6 A1586; Apple, Inc., United States of America), which is hereafter referred to as the smartphone microphone. While measuring cough sounds, the

user was required to hold the bottom of the smartphone in their right hand with the elbow flexed to 90 degrees, the shoulder at 0 degrees, and the elbow internally rotated to 45 degrees (Figure 4.1a, b). Figure 4.1a shows how to hold the smartphone and the location of the microphone. The smartphone screen was directed towards the participant's mouth so that microphone was directed to the body of the user to avoid recording the sound of exhaled air. Figure 1c shows the flowchart for measuring and analysing cough sounds. The cough sound signals are digitized by the smartphone's built-in 16-bit AD converter at a sampling rate of 48 kHz and saved in the native .wav format on the device. The recorded cough sound is then preprocessed as shown in the flowchart in Figure 1c. The digitized cough sound signals are bandpass-filtered between 140 and 2,000 Hz to minimize artefacts caused by heart sounds and muscle interference. Subsequently, the cough sound signals are rectified by calculating their absolute values and smoothed using a 20-ms time window to extract the envelope [42], which represents the cough sound pressure level. The value of the *CPSL* is then calculated from the maximal value of the envelope. The *CPSL* is then substituted into the proposed model, shown in Equation (4.1), to estimate the cough peak flow ($CPS_{proposed}$).

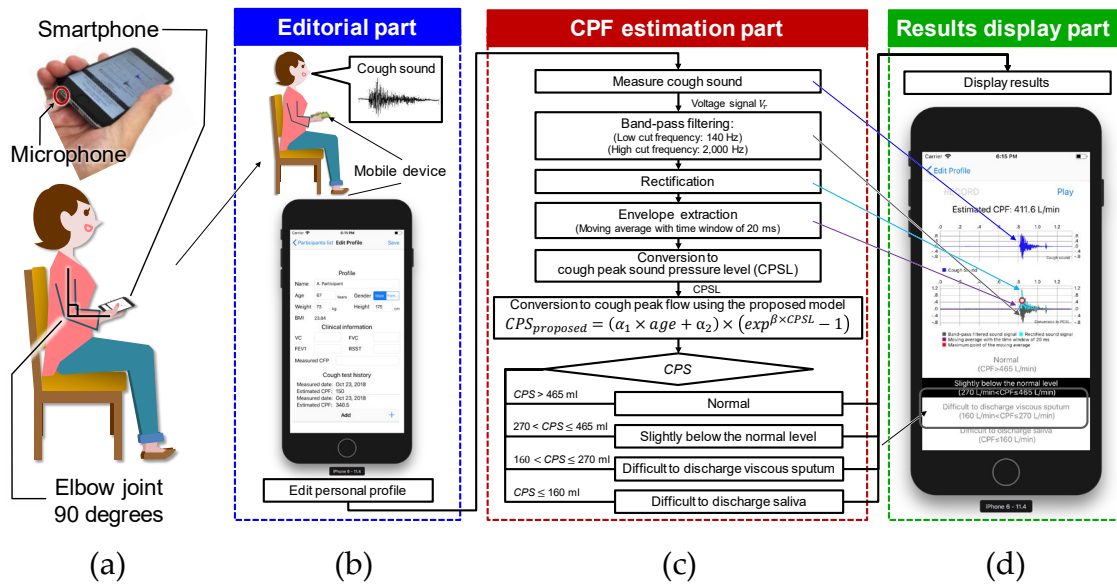


Figure 4.1 Cough sound measurement protocol and software configuration. *CPS* represents the cough peak flow estimated using cough sounds. (a) The posture of a user while recording cough sounds. (b) The user interface for editing a personal profile. (c) The flow chart for cough sound preprocessing and cough peak flow (CPF) estimation. (d) The results display that demonstrates the graphs resulting from signal preprocessing and CPF estimation.

4.2.3 User interface software

The proposed user interface is composed of three parts: the editorial part, the CPF estimation part, and the results display part. The interface starts from the editorial part, which prompts the user to complete their personal profile and proceed to record cough sounds. The CPF estimation part estimates the CPF from the recorded cough sounds using the proposed model. Finally, the estimated CPF is shown in the results display part. Each part of the interface is described below.

Editorial part

Figure 4.2 shows the editorial part. As the initial collection of the participant's

characteristics, this part prompts the user to input their name, age, sex, height and weight. BMI is automatically calculated from the height and weight. The editorial part can also record respiratory functions, such as the vital capacity (VC), forced vital capacity (FVC), forced expiratory volume in one second (FEV₁), measured CPF, and results of an objective swallowing function test, such as the repetitive saliva swallowing test (RSST), which detects patients who experience aspiration [42,79,80]. The bottom of the screen shows the history of the estimated CPFs to inform the user of chronic changes in cough function.

CPF estimation part: The CPF estimation part records the cough sounds, converting the cough sounds into the *CPSL*, and estimates the CPF as described in Sections 4.2.1 and 4.2.2. A user can record cough sounds by pressing the "RECORD" button, as shown in Figure 4.3. The *CPS* is then calculated when the "play" button at the upper right of the screen is pressed, as shown in Figure 4.3.

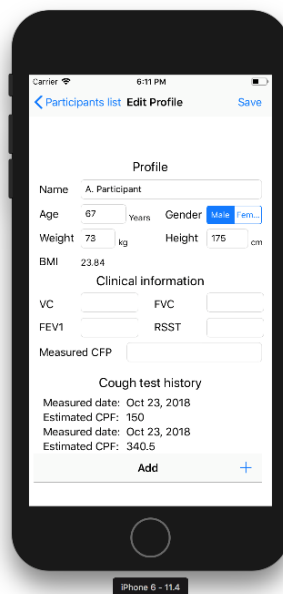


Figure 4.2 Editorial part. This screen prompts the user to complete their personal profile. BMI, body mass index, $BMI = \text{body weight} / \text{height}^2$; VC, vital capacity; FVC, forced vital capacity; FEV₁, forced expiratory volume in 1 s; RSST, repetitive saliva swallowing test.

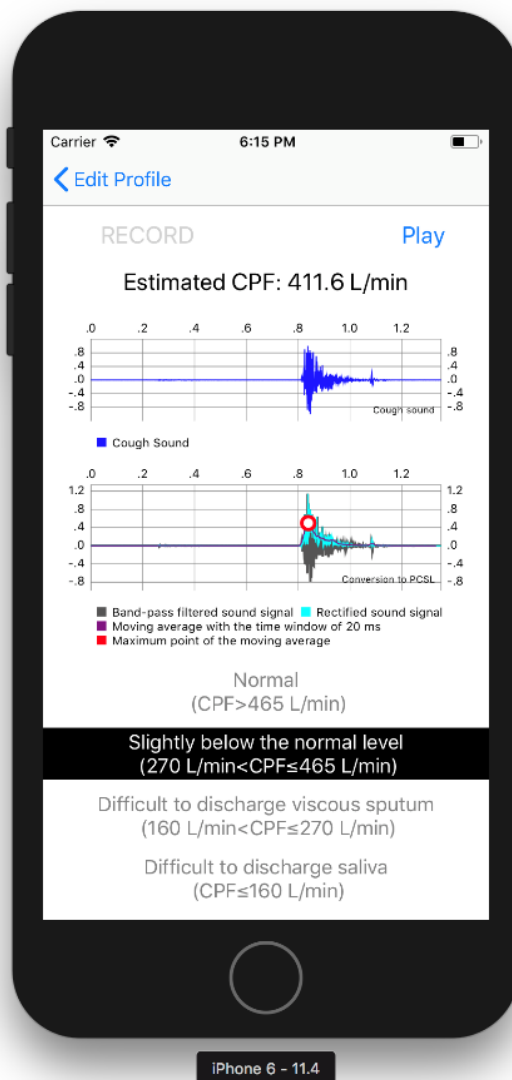


Figure 4.3 Results display part. The blue solid line represents the measured cough sound signal. The light blue solid line represents the rectified sound signal. The purple solid line represents the moving average with a time window of 20 ms. The red dot represents the maximum point of the moving average.

Results display part

Figure 4.3 shows the results display part. The waveform of the cough sounds, the rectified signal, the envelope and the maximum value of the envelope can

be confirmed from the graphs shown in the centre of the screen. The estimated cough peak flow ($CPS_{proposed}$) is classified into four risk levels based on previously reported cut-off values [29-31,79], as shown below and in Figure 4.3:

$CPS_{proposed} > 465$ L/min: Normal level

270 L/min $< CPS_{proposed} \leq 465$ L/min: Slightly below the normal level

160 L/min $< CPS_{proposed} \leq 270$ L/min: Difficult to discharge viscous sputum

$CPS_{proposed} \leq 160$ L/min: Difficult to discharge saliva

4.3 Experiments

4.3.1 Participants

This study was conducted in accordance with the amended declaration of Helsinki. The Hiroshima Cosmopolitan University Institutional Review Board (No. 2015031) approved the protocol, and written informed consent was obtained from all participants. We performed experiments on 33 young participants (21.3 ± 0.4 years) and 25 elderly participants (80.4 ± 6.1 years) (Table 4.1). The participants consisted of self-reported healthy individuals with no previous cardiovascular or pulmonary diseases. Before the cough sound measurements, we measured the %VC, FEV₁, and FVC and excluded those participants with FEV₁/FVC $< 80\%$ and those who could not perform the measurement. As the result, two elderly participants with FEV₁/FVC $< 80\%$ were excluded, representing 3.3% of the all participants.

Table 4.1 Characteristics of the participants.

| Variable | Young participants (<i>n</i> = 33) | Elderly participants (<i>n</i> = 25) | <i>P</i> value |
|--|--|--|----------------|
| Age, years | 21.3 ± 0.4 | 80.4 ± 6.1 | < 0.001 |
| Male sex, <i>n</i> | 20 | 10 | 0.209 |
| Height, cm | 164.6 ± 8.4 | 154.1 ± 8.3 | 0.093 |
| Body weight, kg (male, female) | 58.5 ± 11.6 (64.5 ± 11.3, 51.0 ± 6.2) | 55.1 ± 11.9 (58.6 ± 6.3, 53.4 ± 15.1) | 0.156 |
| BMI, kg/m ² (male, female) | 21.3 ± 0.5 (21.4 ± 0.6, 20.9 ± 0.5) | 23.3 ± 4.1 (22.5 ± 1.6, 24.0 ± 5.2) | 0.216 |
| %VC, % | 97.0 ± 8.9 | 91.5 ± 17.5 | 0.438 |
| FEV ₁ /FVC, % | 90.4 ± 7.6 | 91.8 ± 8.2 | 0.185 |

Values presented are the number of participants or the mean ± S.D. of the corresponding parameters, unless otherwise stated. BMI, body mass index; VC, vital capacity; %VC, vital capacity expressed as a percentage of the predicted value; FEV₁, forced expiratory volume in 1 s; FVC, forced vital capacity.

4.3.2 Methods

Cough flow and sound measurement methods

To measure cough flows, the participants wore a face mask with a flow sensor (Autospiro AS-507; Minato Medical Science Co., Ltd., Osaka, Japan) attached and performed coughing three times in a sitting position. The measurement range of the flow sensor was 0–840 L/min, and the measurement accuracy was within 3% of the indicated value. Hereafter, the measured CPF refers to the cough peak flow calculated from the maximal value obtained from the flow sensor.

To measure cough sounds, the smartphone microphone was used. As explained in Section 2.2., the *CPSL* was calculated to estimate the CPF. The

proposed model was then compared with other possible equation forms to analyse the effects of age, height, weight and BMI on the estimation accuracy. It should be noted that the sex of the participants had a minimal effect on the CPF estimation accuracy, as we have previously reported [72,78]. Hereafter, we denote the CPF estimated by the proposed model as $CPS_{proposed}$ and those estimated by the model shown in Equations (4.2)-(4.6) explained in the following subsections as CPS_x , where the subscript X distinguishes the model used.

Models for age effect analysis

We hypothesized that the $CPSL$ is proportionally affected by age based on a previous study [64]. To validate this hypothesis, we compared the estimation accuracy with that of our previous model, expressed by Equation (4.2), in which the age effect is not included [72,78]. In addition, the proposed model was compared with the models that include the second- (Equation (4.3)) and third-order (Equation (4.4)) terms of the age variable, as follows:

$$CPS_{previous} = \alpha \cdot (exp^{\beta \cdot CPSL} - 1), \quad (4.2)$$

$$CPS_{age2} = (\alpha_{0,(4.3)} + \alpha_{1,(4.3)} \cdot age + \alpha_{2,(4.3)} \cdot age^2) \cdot (exp^{\beta_{(4.3)} \cdot CPSL} - 1), \quad (4.3)$$

$$CPS_{age3} = (\alpha_{0,(4.4)} + \alpha_{1,(4.4)} \cdot age + \alpha_{2,(4.4)} \cdot age^2 + \alpha_{3,(4.4)} \cdot age^3) \cdot (exp^{\beta_{(4.4)} \cdot CPSL} - 1), \quad (4.4)$$

where $\alpha_{0,(Y)}$ to $\alpha_{3,(Y)}$ and $\beta_{(Y)}$ are constant parameters determined by the Levenberg-Marquardt method using the mean square error between the CPS_x and measured CPF as the evaluation function; the subscript Y distinguishes the model. The 95% CIs are also calculated for each parameter. In addition, the

parameters included in Equation (4.2) are determined by calculating the CPS using a previous model, such as $\alpha = 70.98$ and $\beta = 0.022$, based on our previous study [78]. The Wilcoxon signed-rank test was used to compare the absolute error between the previous and proposed models. Spearman's rank correlation coefficient analysis was used to assess the relationship between each CPSx and measured CPF. Absolute reliability was investigated using the Bland-Altman analysis method to detect systematic bias, such as fixed and proportional bias.

Analysis of models for body weight, BMI and height

We verified the effects of body weight, BMI and height on the prediction accuracy because a previous study reported that the CPF can depend on body weight and height [64]. In this study, we hypothesized that the body weight and/or BMI proportionally increases with increasing CPF and that the height proportionally decreases with increasing *CPSL* because taller participants have longer arms and the increased distance between the smartphone microphone held in the hands (Figure 1a) and the mouth attenuates the sound level. We included the terms for body weight, BMI, and height, as follows:

$$CPS_{WB} = (\alpha_{0,(4.1)} + \alpha_{1,(4.1)} \cdot age + \alpha_w \cdot weight + \alpha_B \cdot BMI) \cdot (exp^{\beta_{(4.1)} \cdot CPSL} - 1), \quad (4.5)$$

$$CPS_{height} = (\alpha_{0,(4.1)} + \alpha_{1,(4.1)} \cdot age) \cdot [exp^{\beta_{(4.1)} \cdot \{CPSL + 20 \log(height/d_0)\}} - 1], \quad (4.6)$$

where α_w , α_B , and d_0 are constant parameters determined using the same method described in the previous section; *weight*, *BMI* and *height* represent the participant's body weight, BMI and height, respectively; and $\alpha_{0,(4.1)}$, $\alpha_{1,(4.1)}$ and $\beta_{(4.1)}$ are the same values as those determined for the proposed model. The second term in the exponential function of Equation (4.6) (the height model) represents

the correction term for the attenuation related to the participant's height. A decrease in the sound level L_p can be calculated by the distance (r, r_0) between the sound source and the microphone, as follows:

$$L_p = 20 \log(r/r_0), \quad (4.7)$$

where r_0 and r are constants. Thus, to correct the *CPSL* for additional sound attenuation, *height* was inserted in Equation (6) instead of r . In this analysis, the coefficient of determination and the 95% CI were calculated for comparison with the proposed model (Equation (4.1)).

All statistical tests in this paper assumed a significance level of 0.05, and analyses were performed using G*power (version 3.1.9.2; University Kiel, Germany) and IBM SPSS Statistics 24.0 (IBM, Chicago, IL, USA).

4.4 Results

Parameter determination

Table 4.2 shows the determined parameters. In the proposed model (Equation (4.1)), the coefficients α_0 , α_1 and β are as follows: $a_0 = 42.90$ (95% CI: 7.84 to 77.96), $a_1 = -0.282$ (95% CI: -0.509 to -0.055), and $\beta = 0.028$ (95% CI: 0.020 to 0.037); the determination coefficient of the proposed model is 0.829. In Equations (4.3) and (4.4), the coefficients are determined in the same manner as in the proposed model. Equation (4.3) yielded a determination coefficient of 0.829. The determined parameters are as follows: $a_{0,(4.3)} = 42.32$ (95% CI: 7.15 to 77.50), $a_{1,(4.3)} = -0.212$ (95% CI: -0.713 to 0.289), $a_{2,(4.3)} = -0.001$ (95% CI: -0.006 to 0.004) and $\beta_{(4.3)} = 0.028$ (95% CI, 0.020 to 0.037). The 95% CIs of the coefficients $a_{1,(4.3)}$ and $a_{2,(4.3)}$ in

Equation (3) include 0. Equation (4) yielded a determination coefficient of 0.832. The determined parameters are as follows: $a_{0,(4.4)} = 6.58$ (95% CI: -70.33 to 83.49), $a_{1,(4.4)} = 2.366$ (95% CI: -3.448 to 8.181), $a_{2,(4.4)} = 0.00$ (95% CI: 0.00 to 0.001), $a_{3,(4.4)} = -0.048$ (95% CI: -0.156 to 0.060), and $\beta_{(4.4)} = 0.028$ (95% CI, 0.020 to 0.037). The 95% CIs of all parameters, except for $\beta_{(4.4)}$ in Equation (4.4), include 0. The 95% CI indicates that only $\alpha_{0,Y}$, $\alpha_{1,Y}$ and β_Y are valid parameters because the 95% CIs of the other parameters include 0.

Table 4.2 Determined parameters.

| Model | Parameter | Determined value | Standard error | 95% CI | | Determination coefficient |
|----------------|--------------------|------------------|----------------|--------|--------|---------------------------|
| | | | | Lower | Upper | |
| Equation (4.1) | $\alpha_{0,(4.1)}$ | 42.90 | 17.50 | 7.84 | 77.96 | 0.829 |
| | $\alpha_{1,(4.1)}$ | -0.282 | 0.113 | -0.509 | -0.055 | |
| | $\beta_{(4.1)}$ | 0.028 | 0.004 | 0.020 | 0.037 | |
| Equation (4.3) | $\alpha_{0,(4.3)}$ | 42.32 | 17.54 | 7.15 | 77.50 | 0.829 |
| | $\alpha_{1,(4.3)}$ | -0.212 | 0.250 | -0.713 | 0.289 | |
| | $\alpha_{2,(4.3)}$ | -0.001 | 0.002 | -0.006 | 0.004 | |
| | $\beta_{(4.3)}$ | 0.028 | 0.004 | 0.020 | 0.037 | |
| Equation (4.4) | $\alpha_{0,(4.4)}$ | 6.58 | 38.34 | -70.33 | 83.49 | 0.832 |
| | $\alpha_{1,(4.4)}$ | 2.366 | 2.899 | -3.448 | 8.181 | |
| | $\alpha_{2,(4.4)}$ | 0.000 | 0.00 | 0.00 | 0.001 | |
| | $\alpha_{3,(4.4)}$ | -0.048 | 0.054 | -0.156 | 0.060 | |
| | $\beta_{(4.4)}$ | 0.028 | 0.004 | 0.020 | 0.037 | |

Estimation accuracy

Based on the determined parameters, the CPF estimation accuracy of the proposed model (Equation (4.1)) was verified. Figure 4.4a demonstrates the relationship between each $CPS_{proposed}$ and measured CPF in the young and elderly participants. To compare the CPF estimation accuracy of the proposed and previous models, Figure 4.4b shows a plot of the $CPS_{previous}$ against the measured CPF. Spearman's rank correlation coefficient analysis showed a significant positive correlation between the $CPS_{proposed}$ and measured CPF in both the young participants ($r = 0.780$; $P < 0.001$; power > 0.99) and the elderly participants ($r = 0.750$; $P < 0.001$; power > 0.99). For all participants, the Spearman's rank correlation coefficient is $r = 0.913$, with $P < 0.001$ and power > 0.99 , as shown in Figure 4.4a. In addition, Spearman's rank correlation coefficient analysis showed a significant positive correlation between the $CPS_{previous}$ and CPF (young participants: $r = 0.795$; $P < 0.001$; power > 0.99 , elderly participants: $r = 0.765$; $P < 0.001$; power > 0.99 , all participants: $r = 0.314$; $P = 0.016$; power, 0.68), as shown in Figure 4.4b. Moreover, in young participants, the Wilcoxon signed-rank test showed no significant differences in the absolute error between the $CPS_{proposed}$ and $CPS_{previous}$ (6.19% vs 8.95%, $P = 0.085$) (Figure 5a); however, in the elderly participants and all the participants, the Wilcoxon signed-rank test showed significant differences in the absolute error between the $CPS_{proposed}$ and $CPS_{previous}$ (13.55% vs 90.01%; $P < 0.001$, 9.96% vs 17.92%; $P = 0.001$, respectively) (Figure 4.5b, c). In addition, Figure 4.6 shows the corresponding Bland-Altman plots for the proposed and previous models. Neither model showed fixed bias, but both models showed proportional bias ($r = -0.318$; $P = 0.015$; power, 0.693, $r = -0.523$; $P < 0.001$; power, 0.991, respectively).

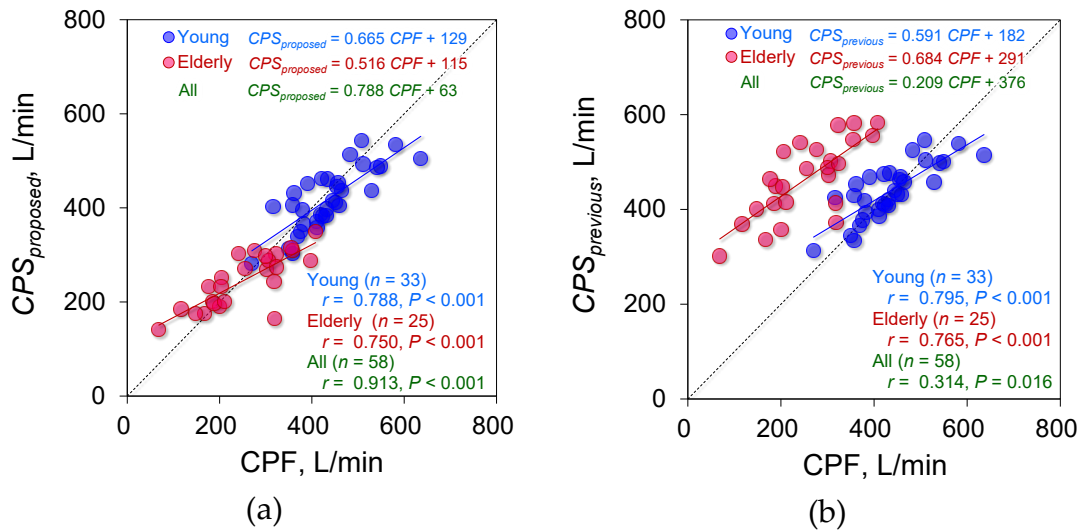


Figure 4.4 Estimation accuracy of $CPS_{proposed}$ and $CPS_{previous}$. (a) The CPF estimated by the proposed model ($CPS_{proposed}$) against the measured CPF. (b) Plot of the CPF estimated by the previous model ($CPS_{previous}$) against the measured CPF. The red and blue circles represent the elderly and young participants, respectively. The linear regression lines are drawn for the groups of young and elderly participants, and the corresponding equations are shown in the upper part of each figure, where the green letters indicate the equation of the regression line for all participants. The right lower side shows the correlation coefficients and P values for each participant group.

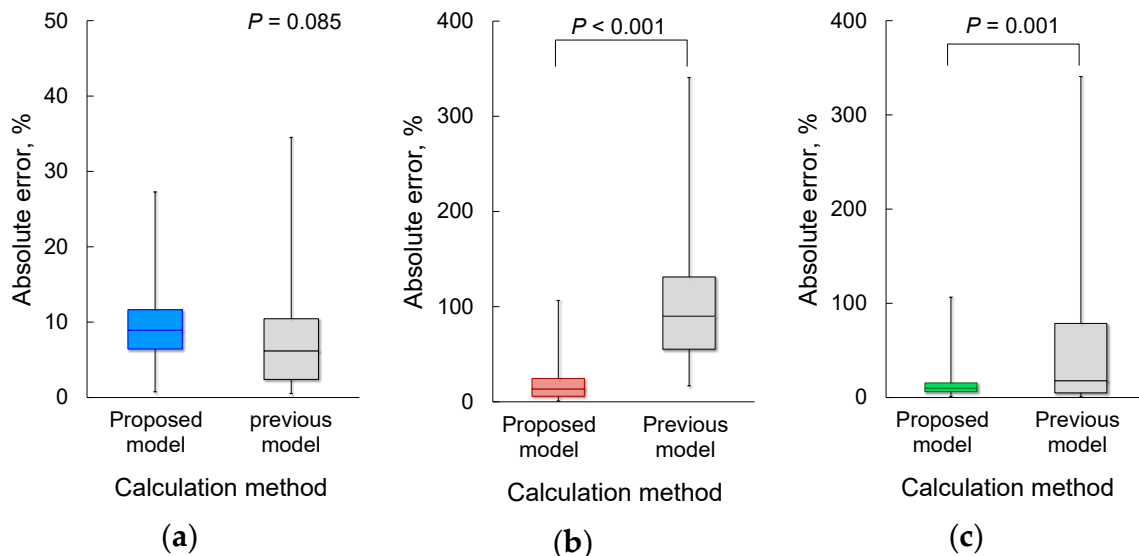


Figure 4.5 Comparison of the absolute error between the proposed and previous models. (a) Young participants, $n = 33$. (b) Elderly participants, $n = 25$. (c) All participants, $n = 58$.

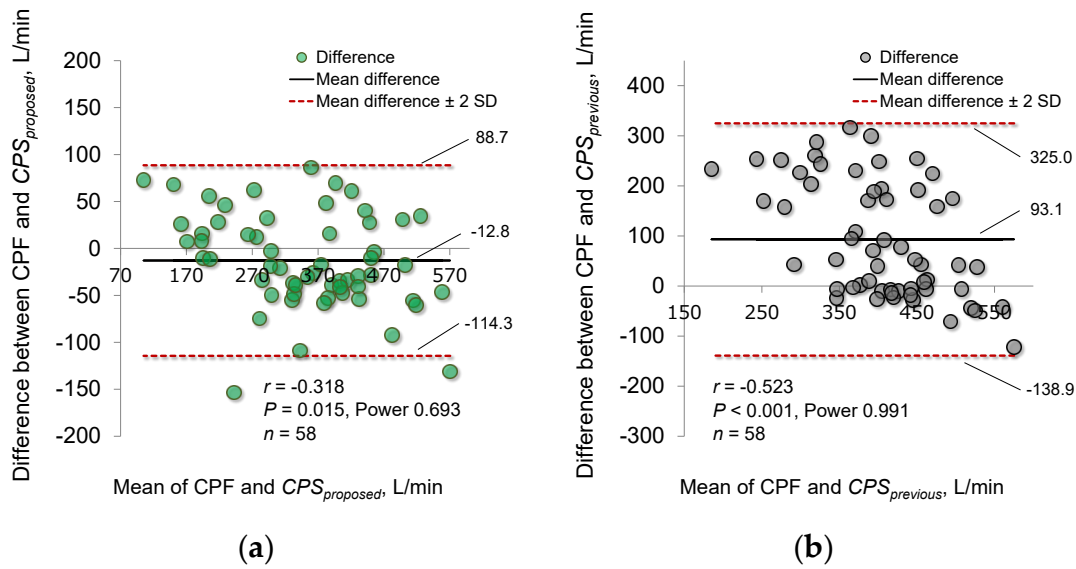


Figure 4.6 Bland-Altman plots of the measured and estimated CPFs. (a) The estimation accuracy of the proposed model ($CPS_{proposed}$). (b) The estimation accuracy of the previous model ($CPS_{previous}$). The horizontal line is the mean of the measured CPF and estimated cough peak flow (CPS_x). The vertical line represents the difference between the measured CPF and CPS_x . The bold black solid lines represent the mean differences between the CPF and CPS_x , and the red dotted lines represent the mean differences ± 2 standard deviations.

Effects of body weight and BMI on CPF estimation accuracy

To consider the effects of body weight and BMI on the CPF estimation accuracy, Equation (4.5), which includes terms for body weight and BMI, was tested. The parameters a_w , a_B and d_0 were determined as explained in Subsection 4.3.2 Method (Models for Age Effect Analysis). The determined parameters are as follows: $a_w = 0.137$ (95% CI: -0.021 to 0.295) and $a_B = -0.303$ (95% CI: -0.717 to 0.110). The 95% CIs of coefficients a_w and a_B in Equation (4.5) include 0, indicating that these parameters are not valid. Equation (4.5) yielded a determination coefficient of 0.839.

Effect of body height on CPF estimation accuracy

The estimation accuracy of Equation (4.6), which includes a term for height in the exponential function, was tested. The determined parameter is $d_0 = 141.6$ (95% CI: 122.8 to 160.5). Equation (4.6) yielded a determination coefficient of 0.833. Spearman's rank correlation coefficient analysis showed a significant positive correlation between the CPS_{height} and measured CPF (young participants: $r = 0.797$; $P < 0.001$; power > 0.99 , elderly participants: $r = 0.772$; $P < 0.001$; power > 0.99 , all participants: $r = 0.916$; $P < 0.001$; power, 1), as shown in Figure 4.7a. In addition, Figure 4.7b shows the corresponding Bland-Altman plot of Equation (4.6). Equation (4.6) did not show fixed or proportional bias ($r = -0.200$; $P = 0.133$).

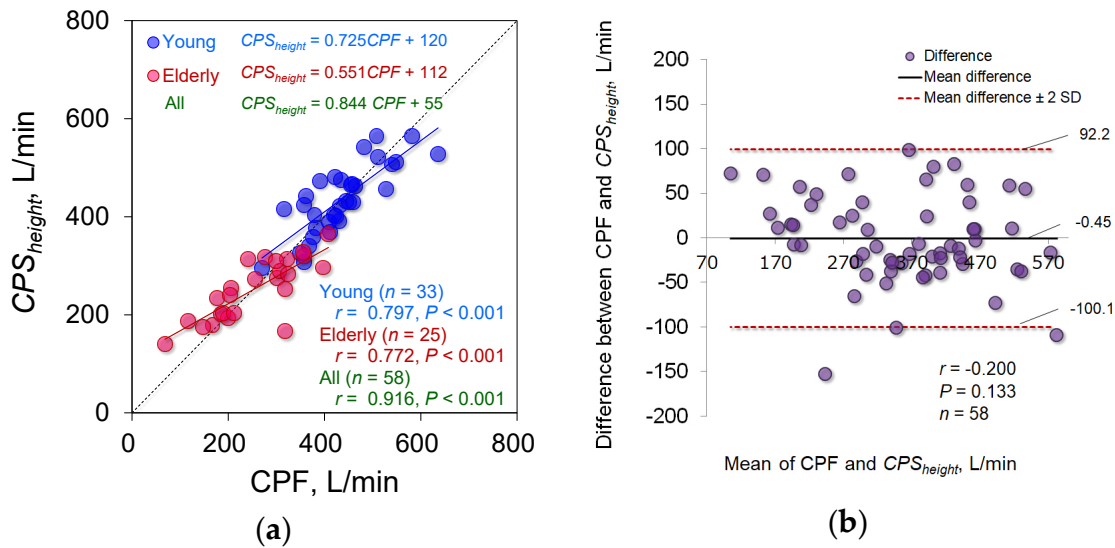


Figure 4.7 Estimation accuracy of CPS_{height} . (a) CPS_{height} against the measured CPF. The linear regression lines are drawn for the young and elderly participant groups, and the corresponding equations are shown in the upper part of each figure, where the green indicates the equation of the regression line for all participants. The right lower part shows the correlation coefficients and p values for each participant group. (b) Bland-Altman plot of the measured CPF and CPS_{height} . The horizontal line is the mean of the measured CPF and CPS_{height} . The vertical line represents the difference between the measured CPF and CPS_{height} . The bold black solid lines represent the mean difference between the measured CPF and each CPS_{height} , and the red dotted lines represent the mean difference ± 2 standard deviation bands.

To compare the estimation accuracy of $CPS_{proposed}$ and CPS_{height} , the absolute error was calculated. The Wilcoxon signed-rank test showed no significant differences in the absolute error between $CPS_{proposed}$ and CPS_{height} (9.96% vs 8.44%; $P = 0.195$), as shown in Figure 4.8.

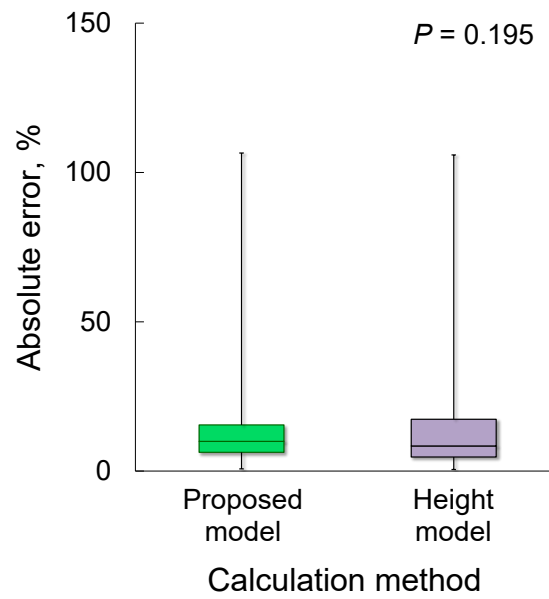


Figure 4.8 Comparison of the absolute error of the proposed and height models. $n = 58$.

Examples of elderly participants

Finally, we performed experiments using the proposed device, implementing the proposed model (Equation (1)). Figures 4.9a and b show examples of two elderly participants in which the measured CPFs were below and above the reference value of 270 L/min.

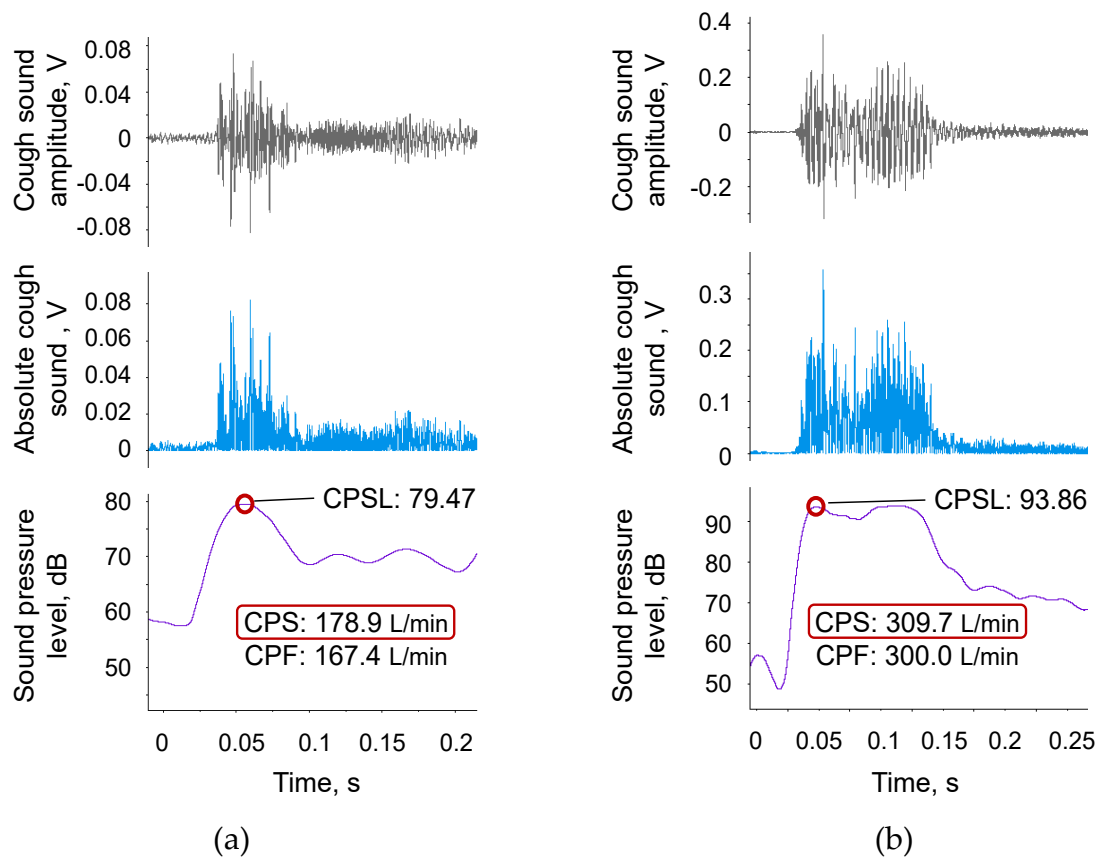


Figure 4.9 Examples of elderly participants. The grey line represents the measured cough sound signal. The light blue solid line represents the bandpass-filtered and rectified sound signal. The purple solid line represents the moving average with a time window of 20 ms. The red circle represents the maximum point of the moving average. (a) Example of a 77-year-old female with a measured CPF below the reference value of 270 L/min. The respiratory function test showed slightly low values of $\%VC=83.5\%$ and $FEV_1/FVC=83.0\%$, but these values exceed the reference value. (b) Example of a 70-year-old male with a measured CPF above the reference value of 270 L/min. The respiratory function test showed normal values of $\%VC=91.6\%$ and $FEV_1/FVC=94.9\%$.

4.5 Discussion

Aiming to establish a method for evaluating cough ability that can be applied in daily clinical practice, we propose a model that can convert cough sounds into CPF values, and we developed a user interface for mobile devices, such as a smartphone, that makes it easy for both patients and caregivers to use the proposed method. To the best of our knowledge, this is the first study to clarify that CPF estimation using cough sounds requires a model involving the age factor. In addition, we found that including the height factor can slightly improve the estimation accuracy.

We hypothesized that age affects the estimation accuracy of the CPF based on the fact that a previous study reported a relationship between the CPF and age [64]. Analysis of the age factor revealed that the proposed model, which includes a first-order term for age (see Equation (4.1)), is sufficient to estimate the CPF from cough sounds (see Figure 4.4a) and that second- or higher-order terms for age (see Equations (4.3) and (4.4)) can be ignored because the 95% CI of the determined parameters included 0 (see Table 4.2). A comparison of the absolute error between the proposed and previous models [72,78] (Equation (4.2)) showed significantly improved estimation accuracy among elderly participants for the proposed model (see Figure 4.4). This finding indicates that age has a major effect on the CPF estimation accuracy. The age factor may also reflect the relationship between the cough strength, vital capacity [62,63,80] and vocal fold function [81-85].

A previous study reported that the CPF depends on body weight and height [64]. Based on this previous study, we tested a model including terms for

body weight and BMI (see Equation (4.5)); however, the 95% CI of the determined parameters of these terms (α_w and α_B) included 0 (see Section 4.3), indicating that *weight* and *BMI* have minimal effects on the CPF estimation accuracy.

A previous study also reported that the distance between the mouth, which is the sound source, and the microphone needs to be less than 30 cm because the recorded cough sounds attenuate with increasing distance from the sound source [72]. In addition, recorded sounds are affected by reflection from walls because sound propagation in a room is a combination of direct and reflected sound waves from surfaces and boundaries in the room [61]. In the context of the daily applicability of the proposed method, the mobile device was handheld (see Figure 4.1a), and we did not precisely specify the distance between the mouth and the microphone. As a result, the median distance between the participant's mouth and the smartphone microphone was approximately 37.50 cm, and the interquartile range was approximately 6.25 cm. This indicates that recorded cough sounds can be influenced by sound reflection and attenuation and that the distance varied among the participants. This could be one reason the Bland-Altman plot of the proposed model (see Figure 4.6a) showed proportional bias. One possible solution is to attach the microphone to the face to maintain a constant distance between the microphone and the sound source [72]. In this study, another solution was tested, in which the height term was included in the CPF estimation model to compensate for the attenuation (see Equation (4.6)) because there was a significant positive linear relationship between the participant's height and the distance between the sound source (participant's mouth) and the microphone ($r = 0.688$; $P < 0.001$; power > 0.99). We

found that this model successfully eliminated the proportional bias (see Figure 4.7b). However, a comparison of the absolute error between the proposed model and the model including the height term showed no significant difference. Considering daily use, we adopted the model proposed in this paper, which does not require measuring the participant's height. However, there is a possibility that the model including the height term is more suitable for different ethnic groups in which height varies greatly, as the participants in this study were Japanese and their height did not drastically vary (see Table 4.1).

A major limitation of this study is that we did not fully consider cough sound frequencies, although previous studies have suggested that breath sounds can be influenced by sound frequencies [86,87]. The estimation accuracy could thus be further improved by considering the frequency domain. In addition, because the proposed method was aimed at the daily evaluation of cough ability and risk screening, it implicitly assumed to be applicable to healthy or close to healthy users. However, we are also expecting a person with a disease or airway mucous to use the proposed method. In this regard, we did not fully consider the effects of disease and airway mucous, since the participants were healthy volunteers. It is thus necessary to verify the proposed method in patients for further clinical application.

4.6 Concluding Remarks

This paper presents a cough strength evaluation based on cough sounds considering the effect of age and designed for daily use in clinical practice along with a custom-designed user interface. The experimental results confirm that the

age term improves the CPF estimation accuracy and that height can also affect the estimation accuracy. This study found that body weight and BMI have minimal effects on the CPF estimation accuracy. This is unexpected result because previous studies [64] reported CPF correlate with body weight. This indicates that cough sound may carry information about body weight and allows CPF estimation without using weight as a parameter; this is a novel fact revealed by this study. The experiment results also revealed that cough strength can be evaluated in elderly people by using the proposed model and device. This finding indicates that the sound quality may change with age, but its effect on CPF estimation can be compensated by adding a proportional age coefficient; this is another novel finding of this study. Toward practical application, we plan to test the efficacy of the proposed model and the user interface software implemented on a mobile device for daily use during in-home care.

Chapter 5

Conclusions

This study proposed a CPF estimation model via cough sound for the development of a novel simple cough strength evaluation method based on the hypothesis that cough sounds are associated with cough flow, and investigated the microphone installation method, the effects of participant's height, weight, BMI, age and microphone type on CPF estimation. We proposed a mobile cough strength evaluation device using the proposed model. The application of the proposed device to elderly people and improvement of the proposed model by considering age were presented in this dissertation.

We proposed a nonlinear model represented by an exponential equation for predicting cough strength in Japanese youths via cough sounds, and investigated the relationship between cough sounds and cough flows and the effects of the measurement condition of cough sound as well as participant's height and gender on CPF estimation accuracy, as presented in Chapter 2. The results confirmed that the proposed model estimated the CPF with high accuracy. The absolute errors between measured CPFs and estimated CPFs were significantly lower when the microphone distance from the participant's mouth

was within 30 cm compared to when the distance exceeded 30 cm. Analysis of the model parameters showed that the estimation accuracy was not affected by the participant's height or gender.

We verified the effects of three types of microphones (in-ear microphone, mini speech microphone, and microphone built-in smartphone) on the CPF estimation accuracy, as presented in Chapter 3. From the non-linear regression analysis results, the determination coefficients were high (greater than 0.7) for the three types of microphones investigated. Furthermore, including the height variable in the revised prediction equation of CPF improved the CPF estimation accuracy of cough sounds recorded using the in-ear and smartphone microphones.

In Chapter 4, we presented a cough strength evaluation device based on cough sounds considering the effect of age, which was designed for daily use in clinical practice along with a custom-designed user interface. Experimental results confirm that the age term improves the CPF estimation accuracy and that height can also affect the estimation accuracy. This study found that body weight and BMI have minimal effects on the CPF estimation accuracy. This is an unexpected result because previous studies reported that CPF correlates with body weight [64]. This indicates that cough sound may carry information on body weight and allows CPF estimation without using weight as a parameter; this is a novel finding of this study. Experimental results also reveal that cough strength can be evaluated in elderly people using the proposed model and device. This finding indicates that the sound quality may change with age, but its effect on CPF estimation can be compensated by adding a proportional age

coefficient; this is another novel finding of this study.

The following are the directions for future research. First, the effect of cough sound frequencies should be considered. Previous studies have suggested that breath sounds can be influenced by sound frequencies [86,87]. The frequency domain of breathing sound is also related to the flow rate as reported in a previous study [18]. Thus, the estimation accuracy can be further improved by considering the frequency domain.

Second, the effect of environmental sound and sound reflection should be also considered because the experiment was conducted in a dedicated room to minimize the influence of surrounding noise, and the participants sat away from the wall to minimize sound reflection. Sound propagation in a room is a combination of direct and reflected sound waves from surfaces and boundaries in the room [61].

Third, it was implicitly assumed to be applicable to healthy or close to healthy users because the proposed method was aimed at the daily evaluation of cough ability and risk screening. However, it is also expected that the proposed method can be applied to a person with a disease or airway mucous. In this regard, we did not fully consider the effects of disease and airway mucous, since the participants in this study were healthy volunteers. It is thus necessary to verify the proposed method in patients for further clinical application.

Moreover, the potential of the cough strength evaluation method via cough sound is explained. The results confirmed a high correlation between measured and estimated CPF, which verified the efficacy of the proposed

method. Moreover, analysing cough sounds can possibly enable the estimation of respiratory functions as well as CPFs because CPFs correlate with respiratory variables such as FVC, FEV₁ and peak expiratory flow rate [64]. We plan to verify the efficacy of the proposed model and the user interface software implemented on a mobile device for daily use during in-home care.

Finally, I am a physical therapist, who has been involved in respiratory care in patients with Duchenne muscular dystrophy for 20 years. During that period, the average life span of them has lengthened to a great extent by advances in respiratory care [88]. However, it is also a reality that many patients are still suffering from disability in the removal of sputum. It is my desire that this dissertation and future works will help reduce their suffering and improve the quality of their life.

Publications concerning this dissertation are listed in the bibliography [72,78,89].

Bibliography

1. Handbook of health and welfare statistics 2014 contents. Japanese ministry of health, labor and welfare.
<http://warp.da.ndl.go.jp/info:ndljp/pid/9518503/www.mhlw.go.jp/english/database/db-hh/xls/1-28.xls> (Accessed on 19th Nov 2018),
2. Teramoto, S.; Fukuchi, Y.; Sasaki, H.; Sato, K.; Sekizawa, K.; Matsuse, T.; Japanese Study Group on Aspiration Pulmonary, D. High incidence of aspiration pneumonia in community- and hospital-acquired pneumonia in hospitalized patients: A multicenter, prospective study in japan. *Journal of the American Geriatrics Society* **2008**, *56*, 577-579.
3. Manabe, T.; Teramoto, S.; Tamiya, N.; Okochi, J.; Hizawa, N. Risk factors for aspiration pneumonia in older adults. *PLoS One* **2015**, *10*, e0140060.
4. Pitts, T.; Troche, M.; Mann, G.; Rosenbek, J.; Okun, M.S.; Sapienza, C. Using voluntary cough to detect penetration and aspiration during oropharyngeal swallowing in patients with parkinson disease. *Chest* **2010**, *138*, 1426-1431.
5. Dosani, R.; Kraman, S.S. Lung sound intensity variability in normal men. A contour phonopneumographic study. *Chest* **1983**, *83*, 628-631.

6. Kraman, S.S. The relationship between airflow and lung sound amplitude in normal subjects. *Chest* **1984**, *86*, 225-229.
7. Shykoff, B.E.; Ploysongsang, Y.; Chang, H.K. Airflow and normal lung sounds. *The American review of respiratory disease* **1988**, *137*, 872-876.
8. Irwin, R.S.; Boulet, L.-P.; Cloutier, M.M.; Fuller, R.; Gold, P.M.; Hoffstein, V.; Ing, A.J.; McCool, F.D.; O'Byrne, P.; Poe, R.H., *et al.* Managing cough as a defense mechanism and as a symptom. *Chest* **1998**, *114*, 133S-181S.
9. Schmit, K.M.; Coeytaux, R.R.; Goode, A.P.; McCrory, D.C.; Yancy, W.S., Jr.; Kemper, A.R.; Hasselblad, V.; Heidenfelder, B.L.; Sanders, G.D. Evaluating cough assessment tools: A systematic review. *Chest* **2013**, *144*, 1819-1826.
10. Korpáš, J.; Tomori, Z. *Cough and other respiratory reflexes*. Karger: 1979.
11. Fink, J.B. Forced expiratory technique, directed cough, and autogenic drainage. *Respir Care* **2007**, *52*, 1210-1221; discussion 1221-1213.
12. Piirilä, P.; Sovijärvi, A.R.A. Objective assessment of cough. *European Respiratory Journal* **1995**, *8*, 1949-1956.
13. Birring, S.S.; Passant, C.; Patel, R.B.; Prudon, B.; Murty, G.E.; Pavord, I.D. Chronic tonsillar enlargement and cough: Preliminary evidence of a novel and treatable cause of chronic cough. *The European respiratory journal* **2004**, *23*, 199-201.
14. French, C.T.; Irwin, R.S.; Fletcher, K.E.; Adams, T.M. Evaluation of a

- cough-specific quality-of-life questionnaire. *Chest* **2002**, *121*, 1123-1131.
15. Birring, S.S.; Prudon, B.; Carr, A.J.; Singh, S.J.; Morgan, M.D.; Pavord, I.D. Development of a symptom specific health status measure for patients with chronic cough: Leicester cough questionnaire (lcq). *Thorax* **2003**, *58*, 339-343.
 16. Prudon, B.; Birring, S.S.; Vara, D.D.; Hall, A.P.; Thompson, J.P.; Pavord, I.D. Cough and glottic-stop reflex sensitivity in health and disease. *Chest* **2005**, *127*, 550-557.
 17. Hsu, J.Y.; Stone, R.A.; Logansinclair, R.B.; Worsdell, M.; Busst, C.M.; Chung, K.F. Coughing frequency in patients with persistent cough - assessment using a 24-hour ambulatory recorder. *European Respiratory Journal* **1994**, *7*, 1246-1253.
 18. Morice, A.H.; Fontana, G.A.; Belvisi, M.G.; Birring, S.S.; Chung, K.F.; Diczpinigaitis, P.V.; Kastelik, J.A.; McGarvey, L.P.; Smith, J.A.; Tatar, M., *et al.* ERS guidelines on the assessment of cough. *The European respiratory journal* **2007**, *29*, 1256-1276.
 19. Birring, S.S.; Matos, S.; Patel, R.B.; Prudon, B.; Evans, D.H.; Pavord, I.D. Cough frequency, cough sensitivity and health status in patients with chronic cough. *Respir Med* **2006**, *100*, 1105-1109.
 20. Su, W.L.; Chen, Y.H.; Chen, C.W.; Yang, S.H.; Su, C.L.; Perng, W.C.; Wu, C.P.; Chen, J.H. Involuntary cough strength and extubation outcomes for patients in an icu. *Chest* **2010**, *137*, 777-782.

21. Duan, J.; Zhou, L.; Xiao, M.; Liu, J.; Yang, X. Semiquantitative cough strength score for predicting reintubation after planned extubation. *American journal of critical care : an official publication, American Association of Critical-Care Nurses* **2015**, *24*, e86-90.
22. Bai, L.; Duan, J. Use of cough peak flow measured by a ventilator to predict re-intubation when a spirometer is unavailable. *Respir Care* **2017**, *62*, 566-571.
23. Bach, J.R. Update and perspectives on noninvasive respiratory muscle aids. Part 1: The inspiratory aids. *Chest* **1994**, *105*, 1230-1240.
24. Finder, J.D.; Birnkrant, D.; Carl, J.; Farber, H.J.; Gozal, D.; Iannaccone, S.T.; Kovesi, T.; Kravitz, R.M.; Panitch, H.; Schramm, C., *et al.* Respiratory care of the patient with duchenne muscular dystrophy: Ats consensus statement. *Am J Respir Crit Care Med* **2004**, *170*, 456-465.
25. Chatwin, M.; Toussaint, M.; Goncalves, M.R.; Sheers, N.; Mellies, U.; Gonzales-Bermejo, J.; Sancho, J.; Fauroux, B.; Andersen, T.; Hov, B., *et al.* Airway clearance techniques in neuromuscular disorders: A state of the art review. *Respir Med* **2018**, *136*, 98-110.
26. Hull, J.; Aniapravan, R.; Chan, E.; Chatwin, M.; Forton, J.; Gallagher, J.; Gibson, N.; Gordon, J.; Hughes, I.; McCulloch, R., *et al.* British thoracic society guideline for respiratory management of children with neuromuscular weakness. *Thorax* **2012**, *67 Suppl 1*, i1-40.
27. Strickland, S.L.; Rubin, B.K.; Drescher, G.S.; Haas, C.F.; O'Malley, C.A.;

- Volsko, T.A.; Branson, R.D.; Hess, D.R. Aarc clinical practice guideline: Effectiveness of nonpharmacologic airway clearance therapies in hospitalized patients. *Respir Care* **2013**, *58*, 2187-2193.
28. Akashiba, T.; Ishikawa, Y.; Ishihara, H.; Imanaka, H.; Ohi, M.; Ochiai, R.; Kasai, T.; Kimura, K.; Kondoh, Y.; Sakurai, S., *et al.* The japanese respiratory society noninvasive positive pressure ventilation (nppv) guidelines (second revised edition). *Respiratory investigation* **2017**, *55*, 83-92.
29. Bach, J.R. Amyotrophic lateral sclerosis: Predictors for prolongation of life by noninvasive respiratory aids. *Arch Phys Med Rehabil* **1995**, *76*, 828-832.
30. Bach, J.R.; Saporito, L.R. Criteria for extubation and tracheostomy tube removal for patients with ventilatory failure. A different approach to weaning. *Chest* **1996**, *110*, 1566-1571.
31. Bach, J.R.; Ishikawa, Y.; Kim, H. Prevention of pulmonary morbidity for patients with duchenne muscular dystrophy. *Chest* **1997**, *112*, 1024-1028.
32. Yawata, A.; Tsubaki, A.; Yawata, H.; Takai, H.; Matsumoto, K.; Takehara, N.; Kobayashi, R. Voluntary cough intensity and its influencing factors differ by sex in community-dwelling adults. *Therapeutic advances in respiratory disease* **2017**, *11*, 427-433.
33. Bianchi, C.; Baiardi, P.; Khirani, S.; Cantarella, G. Cough peak flow as a predictor of pulmonary morbidity in patients with dysphagia. *American journal of physical medicine & rehabilitation* **2012**, *91*, 783-788.

34. Riquelme, R.; Torres, A.; El-Ebiary, M.; de la Bellacasa, J.P.; Estruch, R.; Mensa, J.; Fernandez-Sola, J.; Hernandez, C.; Rodriguez-Roisin, R. Community-acquired pneumonia in the elderly: A multivariate analysis of risk and prognostic factors. *Am J Respir Crit Care Med* **1996**, *154*, 1450-1455.
35. Ebihara, S.; Sekiya, H.; Miyagi, M.; Ebihara, T.; Okazaki, T. Dysphagia, dystussia, and aspiration pneumonia in elderly people. *Journal of thoracic disease* **2016**, *8*, 632-639.
36. Huang, C.-T.; Yu, C.-J. Conventional weaning parameters do not predict extubation outcome in intubated subjects requiring prolonged mechanical ventilation. *Respiratory Care* **2013**, *58*, 1307-1314.
37. Thille, A.W.; Boissier, F.; Ben Ghezala, H.; Razazi, K.; Mekontso-Dessap, A.; Brun-Buisson, C. Risk factors for and prediction by caregivers of extubation failure in icu patients: A prospective study. *Critical care medicine* **2015**, *43*, 613-620.
38. Toop, L.J.; Dawson, K.P.; Thorpe, C.W. A portable system for the spectral analysis of cough sounds in asthma. *The Journal of asthma : official journal of the Association for the Care of Asthma* **1990**, *27*, 393-397.
39. Thorpe, C.; Toop, L.; Dawson, K. Towards a quantitative description of asthmatic cough sounds. *European Respiratory Journal* **1992**, *5*, 685-692.
40. Murata, A.; Taniguchi, Y.; Hashimoto, Y.; Kaneko, Y.; Takasaki, Y.; Kudoh, S. Discrimination of productive and non-productive cough by sound

- analysis. *Intern Med* **1998**, *37*, 732-735.
41. Hashimoto, Y.; Murata, A.; Mikami, M.; Nakamura, S.; Yamanaka, E.; Kudoh, S. Influence of the rheological properties of airway mucus on cough sound generation. *Respirology (Carlton, Vic.)* **2003**, *8*, 45-51.
 42. Murata, A.; Ohota, N.; Shibuya, A.; Ono, H.; Kudoh, S. New non-invasive automatic cough counting program based on 6 types of classified cough sounds. *Intern Med* **2006**, *45*, 391-397.
 43. Rece, C.A.; Cherry, A.C., Jr.; Reece, A.T.; Hatcher, T.B.; Diehl, A.M. Tape recorder for evaluation of coughs in children. *American journal of diseases of children (1960)* **1966**, *112*, 124-128.
 44. Loudon, R.G.; Brown, L.C. Cough frequency in patients with respiratory disease. *The American review of respiratory disease* **1967**, *96*, 1137-1143.
 45. Van Hirtum, A.; Berckmans, D. Automated recognition of spontaneous versus voluntary cough. *Medical engineering & physics* **2002**, *24*, 541-545.
 46. Van Hirtum, A.; Berckmans, D. Assessing the sound of cough towards vocality. *Medical engineering & physics* **2002**, *24*, 535-540.
 47. Srour, N.; LeBlanc, C.; King, J.; McKim, D.A. Lung volume recruitment in multiple sclerosis. *PLoS One* **2013**, *8*, e56676.
 48. LoMauro, A.; Aliverti, A.; Mastella, C.; Arnoldi, M.T.; Banfi, P.; Baranello, G. Spontaneous breathing pattern as respiratory functional outcome in children with spinal muscular atrophy (sma). *PLoS One* **2016**, *11*,

- e0165818.
49. Benditt, J.O.; Boitano, L.J. Pulmonary issues in patients with chronic neuromuscular disease. *Am J Respir Crit Care Med* **2013**, *187*, 1046-1055.
 50. Sancho, J.; Servera, E.; Diaz, J.; Marin, J. Predictors of ineffective cough during a chest infection in patients with stable amyotrophic lateral sclerosis. *Am J Respir Crit Care Med* **2007**, *175*, 1266-1271.
 51. Duan, J.; Liu, J.; Xiao, M.; Yang, X.; Wu, J.; Zhou, L. Voluntary is better than involuntary cough peak flow for predicting re-intubation after scheduled extubation in cooperative subjects. *Respir Care* **2014**, *59*, 1643-1651.
 52. Smailes, S.T.; McVicar, A.J.; Martin, R. Cough strength, secretions and extubation outcome in burn patients who have passed a spontaneous breathing trial. *Burns : journal of the International Society for Burn Injuries* **2013**, *39*, 236-242.
 53. Larson, S.; Comina, G.; Gilman, R.H.; Tracey, B.H.; Bravard, M.; Lopez, J.W. Validation of an automated cough detection algorithm for tracking recovery of pulmonary tuberculosis patients. *PLoS One* **2012**, *7*, e46229.
 54. Sumner, H.; Woodcock, A.; Kolsum, U.; Dockry, R.; Lazaar, A.L.; Singh, D.; Vestbo, J.; Smith, J.A. Predictors of objective cough frequency in chronic obstructive pulmonary disease. *Am J Respir Crit Care Med* **2013**, *187*, 943-949.
 55. Ing, A.J.; Ngu, M.C.; Breslin, A.B. Pathogenesis of chronic persistent cough

- associated with gastroesophageal reflux. *Am J Respir Crit Care Med* **1994**, *149*, 160-167.
56. Lee, K.K.; Matos, S.; Evans, D.H.; White, P.; Pavord, I.D.; Birring, S.S. A longitudinal assessment of acute cough. *Am J Respir Crit Care Med* **2013**, *187*, 991-997.
57. Birring, S.S.; Fleming, T.; Matos, S.; Raj, A.A.; Evans, D.H.; Pavord, I.D. The leicester cough monitor: Preliminary validation of an automated cough detection system in chronic cough. *The European respiratory journal* **2008**, *31*, 1013-1018.
58. Spinou, A.; Birring, S.S. An update on measurement and monitoring of cough: What are the important study endpoints? *Journal of thoracic disease* **2014**, *6*, S728-734.
59. Taylor, T.E.; Lacalle Muls, H.; Costello, R.W.; Reilly, R.B. Estimation of inhalation flow profile using audio-based methods to assess inhaler medication adherence. In *PloS one*, 2018; Vol. 13, p e0191330.
60. National health in 2016 and nutritional investigation report. Japanese ministry of health, labor and welfare.
<https://www.mhlw.go.jp/bunya/kenkou/eiyou/dl/h28-houkoku-05.pdf>
(Accessed on 7th July 2018),
61. Shafieian, M.; Kashani, F.H. Effect of diffusive and nondiffusive surfaces combinations on sound diffusion. *Acoustical Physics* **2010**, *56*, 342-347.
62. Baldwin, E.D.; Cournand, A.; Richards, D.W., Jr. Pulmonary insufficiency;

- physiological classification, clinical methods of analysis, standard values in normal subjects. *Medicine* **1948**, *27*, 243-278.
63. Berglund, E.; Birath, G.; Bjure, J.; Grimby, G.; Kjellmer, I.; Sandqvist, L.; Soderholm, B. Spirometric studies in normal subjects. I. Forced expirograms in subjects between 7 and 70 years of age. *Acta medica Scandinavica* **1963**, *173*, 185-192.
64. Bianchi, C.; Baiardi, P. Cough peak flows: Standard values for children and adolescents. *American journal of physical medicine & rehabilitation* **2008**, *87*, 461-467.
65. Reyes, B.A.; Reljin, N.; Chon, K.H. Tracheal sounds acquisition using smartphones. *Sensors (Basel)* **2014**, *14*, 13830-13850.
66. Lee, K.K.; Matos, S.; Ward, K.; Rafferty, G.F.; Moxham, J.; Evans, D.H.; Birring, S.S. Sound: A non-invasive measure of cough intensity. *BMJ open respiratory research* **2017**, *4*, e000178.
67. Fuller, R.W.; Jackson, D.M. Physiology and treatment of cough. *Thorax* **1990**, *45*, 425-430.
68. Hegland, K.W.; Okun, M.S.; Troche, M.S. Sequential voluntary cough and aspiration or aspiration risk in parkinson's disease. *Lung* **2014**, *192*, 601-608.
69. Smith Hammond, C.A.; Goldstein, L.B.; Zajac, D.J.; Gray, L.; Davenport, P.W.; Bolser, D.C. Assessment of aspiration risk in stroke patients with quantification of voluntary cough. *Neurology* **2001**, *56*, 502-506.

70. Bach, J.R. Update and perspective on noninvasive respiratory muscle aids. Part 2: The expiratory aids. *Chest* **1994**, *105*, 1538-1544.
71. William Thorpe, C.; Richard Fright, W.; Toop, L.J.; Dawson, K.P. A microcomputer-based interactive cough sound analysis system. *Computer Methods and Programs in Biomedicine* **1991**, *36*, 33-43.
72. Umayahara, Y.; Soh, Z.; Sekikawa, K.; Kawae, T.; Otsuka, A.; Tsuji, T. Estimation of cough peak flow using cough sounds. *Sensors* **2018**, *18*, 2381.
73. Bland, J.M.; Altman, D.G. Statistical methods for assessing agreement between two methods of clinical measurement. *Lancet (London, England)* **1986**, *1*, 307-310.
74. Beardsmore, C.S.; Wimpress, S.P.; Thomson, A.H.; Patel, H.R.; Goodenough, P.; Simpson, H. Maximum voluntary cough: An indication of airway function. *Bulletin europeen de physiopathologie respiratoire* **1987**, *23*, 465-472.
75. Beardsmore, C.S.; Park, A.; Wimpress, S.P.; Thomson, A.H.; Simpson, H. Cough flow-volume relationships in normal and asthmatic children. *Pediatric pulmonology* **1989**, *6*, 223-231.
76. Matos, S.; Birring, S.S.; Pavord, I.D.; Evans, D.H. Detection of cough signals in continuous audio recordings using hidden markov models. *IEEE transactions on bio-medical engineering* **2006**, *53*, 1078-1083.
77. Matos, S.; Birring, S.S.; Pavord, I.D.; Evans, D.H. An automated system for 24-h monitoring of cough frequency: The leicester cough monitor. *IEEE*

- transactions on bio-medical engineering* **2007**, *54*, 1472-1479.
78. Umayahara, Y.; Soh, Z.; Ozaki, T.; Murakami, T.; Otsuka, A.; Tsuji, T. In *Ability to cough can be evaluated through cough sounds: An experimental investigation of effects of microphone type on accuracy*, 2017 IEEE/SICE International Symposium on System Integration (SII), 11-14 Dec. 2017, 2017; pp 936-941.
79. Sivasothy, P.; Brown, L.; Smith, I.E.; Shneerson, J.M. Effect of manually assisted cough and mechanical insufflation on cough flow of normal subjects, patients with chronic obstructive pulmonary disease (copd), and patients with respiratory muscle weakness. *Thorax* **2001**, *56*, 438-444.
80. Smith, J.A.; Aliverti, A.; Quaranta, M.; McGuinness, K.; Kelsall, A.; Earis, J.; Calverley, P.M. Chest wall dynamics during voluntary and induced cough in healthy volunteers. *The Journal of physiology* **2012**, *590*, 563-574.
81. Bonilha, H.S.; Gerlach, T.T.; Sutton, L.E.; Dawson, A.E.; McGrattan, K.; Nietert, P.J.; Deliyski, D.D. Efficacy of six tasks to clear laryngeal mucus aggregation. *Journal of voice : official journal of the Voice Foundation* **2017**, *31*, 254.e211-254.e215.
82. Britton, D.; Benditt, J.O.; Merati, A.L.; Miller, R.M.; Stepp, C.E.; Boitano, L.; Hu, A.; Ciol, M.A.; Yorkston, K.M. Associations between laryngeal and cough dysfunction in motor neuron disease with bulbar involvement. *Dysphagia* **2014**, *29*, 637-646.
83. Makiyama, K.; Yoshihashi, H.; Park, R.; Shimazaki, N.; Nakai, M.

- Assessment of phonatory function by the airway interruption method: Age-related changes. *Otolaryngology--head and neck surgery : official journal of American Academy of Otolaryngology-Head and Neck Surgery* **2006**, *134*, 407-412.
84. Nishio, M.; Niimi, S. Changes in speaking fundamental frequency characteristics with aging. *The Japan Journal of Logopedics and Phoniatrics* **2005**, *46*, 136-144.
85. Goy, H.; Fernandes, D.N.; Pichora-Fuller, M.K.; van Lieshout, P. Normative voice data for younger and older adults. *Journal of voice : official journal of the Voice Foundation* **2013**, *27*, 545-555.
86. Gross, V.; Dittmar, A.; Penzel, T.; SchÜttler, F.; Wichert, P.v. The relationship between normal lung sounds, age, and gender. *Am J Respir Crit Care Med* **2000**, *162*, 905-909.
87. Duffin, J.M. Puerile respiration: Laennec's stethoscope and the physiology of breathing. *Transactions & studies of the College of Physicians of Philadelphia* **1991**, *13*, 125-145.
88. Ishikawa, Y.; Miura, T.; Ishikawa, Y.; Aoyagi, T.; Ogata, H.; Hamada, S.; Minami, R. Duchenne muscular dystrophy: Survival by cardio-respiratory interventions. *Neuromuscular Disorders* **2011**, *21*, 47-51.
89. Umayahara, Y.; Soh, Z.; Sekikawa, K.; Kawae, T.; Otsuka, A.; Tsuji, T. A mobile cough strength evaluation device using cough sounds. *Sensors* **2018**, *18*, 3810.

Acknowledgements

My deepest appreciation goes to my advisor, Professor Toshio Tsuji, Biological Systems Engineering Laboratory, Division of Electrical, Systems and Mathematical Engineering, Institute of Engineering, Hiroshima University, whose comments and suggestions were of inestimable value for my study. He taught me in various research fields of biological signal analysis, welfare and medical applications. His serious and passionate attitude for research has been an excellent example to me.

I would like to thank the committee members, Professor Idaku Ishii and Professor Toru Yamamoto, Division of Electrical, Systems and Mathematical Engineering, Institute of Engineering, Hiroshima University, for their invaluable suggestions and discussions on this dissertation.

Special thanks also go to Assistant Professor Zu Soh, Biological Systems Engineering Laboratory, Division of Electrical, Systems and Mathematical Engineering, Institute of Engineering, Hiroshima University, who provided technical assistance and sincere encouragement.

I am deeply grateful to Professor Yuichi Kurita and all the members of the Biological Systems Engineering Laboratory, Hiroshima University, for their encouragement and support.

I would like to express my gratitude to Associate Professor Kiyokazu Sekikawa, Division of Physical Analysis and Therapeutic Sciences, Institute of Biomedical and Health Sciences, Hiroshima University, who provided constructive comments and warm encouragement.

I owe my gratitude to Mr. Toshihiro Kawae, Division of Rehabilitation, Department of Clinical Support, Hiroshima University Hospital, Dr. Yoshihiko Ando, Mr. Seiichi Yoshikawa and Ms. Nozomi Yamasaki, R PLUS CO. Ltd., for their support.

I would like to express my gratitude to Dean Toshiaki Furusawa, President Nobuoki Kohno, Professor Masahiko Fujimura and Professor Seiji Togashi, Hiroshima Cosmopolitan University, for allowing me to attend graduate school.

I would like to express my sincere appreciation to Professor Akira Otsuka, for his generous support and warm encouragement. Without his guidance and persistent help, this dissertation would not have been possible.

Finally, I would also like to express my heartfelt gratitude to my family for their dedicated support and warm encouragements. Special thanks to my wife for all the support.

My Ph.D. study was supported in part by Japan Society for the Promotion of Science (JSPS) KAKENHI Grant Number 16K16475.